# OBSERVATIONS AND ANALYSIS OF THE CONTACT BINARY H235 IN THE OPEN CLUSTER NGC 752[1]

E. F. MILONE, C. R. STAGG, B. A. SUGARS,[2] AND J. R. MCVEAN

Department of Physics and Astronomy, Rothney Astrophysical Observatory, The University of Calgary, 2500 University Dr., NW, Calgary, AB, T2N 1N4, Canada
Electronic mail: milone@acs.ucalgary.ca

S. J. SCHILLER

Department of Physics, South Dakota State University, Box 2219, Brookings, South Dakota 57007-0395
Electronic mail: schilles@mg.sdstate.edu

J. KALLRATH

BASF-AG, ZXA/ZC, Kaiser Wilhelm Strasse 52, D-67056, Ludwigshafen, Federal Republic of Germany, and Astronomische Institute der Universität Bonn, Auf dem Hügel 71, D-53121 Bonn, Federal Republic of Germany
Electronic mail: kallrath@zx.basf-ag.de

D. H. BRADSTREET

Department of Physical Sciences, Eastern College, St. Davids, Pennsylvania 19087-3696
Electronic mail: bradstreet@ucis.vill.edu

*Received 1993 December 30; revised 1994 July 29*

## ABSTRACT

The short-period variable star Heinemann 235 in the open cluster NGC 752 has been identified as a contact binary with a variable period of about $0^d.4118$. *BVRI* light curves and radial velocity curves have been obtained and analyzed with enhanced versions of the Wilson–Devinney light curve program. We find that the system is best modeled as an A-type W UMa system, with a contact parameter of $0.21\pm0.11$. The masses of the components are found to be $1.18\pm0.17$ and $0.24\pm0.04\ \mathcal{M}_\odot$, with bolometric magnitudes of $3.60\pm0.10$ and $5.21\pm0.13$, for the hotter (6500 K, assumed) and cooler (6421 K) components, respectively, with $\Delta T=79\pm25$ K. The distance to the binary is established at $381\pm17$ pc. H235 becomes one of a relatively small number of open-cluster contact systems with detailed light curve analysis for which an age may be estimated. If it is coeval with the cluster, and with the detached eclipsing and double-lined spectroscopic binary H219 (DS And), H235 is ~1.8 Gyr old, and may provide a fiducial point for the evolution of contact systems. There is, however, evidence for dynamical evolution of the cluster and the likelihood of weak interactions over the age of the binary precludes the determination of its initial state with certainty.

## 1. INTRODUCTION

The study of binaries in clusters is a royal road to knowledge of both the clusters and the binary stars they may contain. This road is especially lined with riches if the binaries are eclipsing and double-lined spectroscopic binaries. The importance of such binaries has been discussed in the contexts of the distance scale (Milone & Schiller 1988), star cluster evolution (Milone & Schiller 1991), and binary star studies (Schiller 1986, and papers cited below). In this paper we continue our study of the eclipsing binaries in the galactic cluster NGC 752 begun by Schiller & Milone (1988, hereafter referred to as SM88).

A previous object of study in this cluster was the double-lined spectroscopic and eclipsing binary DS Andromedae ($01^h54^m47^s$; $+37°49'53''$ 1950.0)=Heinemann (1926) 219 =Rohlfs & Vanýsek (1961) 79=Stock (1985) 291=Francic (1989) 260=Platais (1991) 897 (hereafter designation identifiers will be H, RV, S, F, and P, respectively). In the case of DS And, the "royal road" was regal indeed, since it was demonstrated (SM88) that the binary system was in the cluster and that its components most likely evolved independently of each other; such a condition allows tests of model isochrones drawn through their separate positions on the CMD and thus provides a means to explore the age and chemical composition of the cluster. Before discussing the new binary study, we reprise and update the results of the study of DS And, and begin with a brief review of cluster properties.

The cluster NGC 752 (OC1 363 of Ruprecht *et al.* 1988) is an open cluster of intermediate age. Investigations of the age of the cluster by application of theoretical isochrones have been carried out by Hardy (1979), Twarog (1983), and by SM88, who made use of Cannon's (1970) CMD which extends down to ZAMS stars, and the isochrones of VandenBerg (1985). A thorough review of all previous NGC 752 photometry, including work in the Strömgren, Johnson, DDO, Geneva, and Washington systems, has now been done

[1]Publication of the Rothney Astrophysical Observatory No. 67.
[2]Present address: CISTS, York University, 4700 Keele St., North York, ON, M3J 1P3, Canada

 0004-6256/95/109(1)/359/19/$0.90  

by Daniel *et al.* (1994) and need not be repeated here. The SM88 value[3] was

$$\tau = 2.0 \pm 0.2 \times 10^9 \text{ yr},$$

under the assumptions $E_{(B-V)}=0.03$ and [Fe/H]=0.0. In the same investigation the distance of the cluster was determined to be

$$(V-M_V)_0 = 7.9 \pm 0.2,$$

in agreement with the distance modulus found from the absolute parameters for the binary:

$$(V-M_V)_0 = 8.17 \pm 0.15.$$

Daniel *et al.* (1994) adopt [Fe/H]$=-0.15\pm0.05$ and $E_{(B-V)}=0.035\pm0.005$, and conclude, from intermediate-band photometry and main sequence fitting, that $(m-M)_0 = 8.25\pm0.10$. They also conclude from classical isochrone fitting that $\tau=1.9\pm0.2$ Gyr and from convective overshoot isochrones, $\tau=1.7\pm0.1$ Gyr.

SM88 demonstrated that DS And was a *bone fide* member of NGC 752 on the basis of a previous proper motion study (Ebbighausen 1939), radial velocity studies (Rebeirot 1970) of the cluster, and the (SM88) radial velocity data of DS And. Subsequent proper motion studies by Francic (1989) and Platais (1991) confirm this assessment. DS And has the following recent measured mean proper motion values:

Francic (1989): $\mu_x = 0\farcs00 \pm 0\farcs01$,
$\mu_y = -0\farcs08 \pm 0\farcs03$; $P \geq 99\%$,

Platais (1991): $\mu_x = 0\farcs0079$,
$\mu_y = -0\farcs0064$; $P = 99\%$,

where Francic's proper motions are given in arcsec/century. Platais indicates that a typical external uncertainty for stars at this range from the cluster center and of this brightness is less than $\sim 0\farcs0015$ yr$^{-1}$. The systemic velocity was determined by SM88 to be $+2.5\pm2.0$ km s$^{-1}$, consistent with membership (see Sec. 4). The positions on the color magnitude diagram (hereafter CMD), and the derived distance of the system further confirmed its membership. The principal conclusion of SM88 was that the components of this system had evolved independently, without substantive mass loss or exchange, so that their properties were reliable guides to a study of the cluster. This brings us to H235, which does not fit that category of binary, but thanks to the studies of NGC 752 and of DS Andromedae, it was thought, it could be studied with the assumed advantages of known age and determinable chemical composition.

Heinemann 235 (Heinemann 1926), hereafter H235, is centrally located in the field of NGC 752 at $01^h53^m01^s$, $+37°34'$ (1950.0). Other designations of H235 have been: S310, F279, and P950; in Cannon's (1968) study it is no. 118 and in Rebeirot's (1970) radial velocity study, it is star 215 (hereafter prefixed with R). Its variability was noted by Johnson (1953) based on two discordant magnitude observations. Crawford & Barnes (1970) place H235 in a list of stars which are "binaries, peculiar, or have discordant observations." Twarog (1983) concluded that H235 was probably a binary based on its location in the CMD. Ebbighausen (1939) assigned H235 a cluster membership class 1, corresponding to a high probability of membership, on the basis of proper motions. New proper motion data bear out this assessment:

Ebbighausen (1936): $\mu_x = +0\farcs004$,
$\mu_y = -0\farcs004$,

Francic (1989): $\mu_x = -0\farcs05 \pm 0\farcs05$,
$\mu_y = -0\farcs05 \pm 0\farcs04$; $P \geq 99\%$,

Platais (1991): $\mu_x = 0\farcs0073$,
$\mu_y = -0\farcs0065$; $P = 99\%$,

where, again, Francic's proper motions are in arcsec/century. Platais indicates that a typical external uncertainty for stars at this range from cluster center and brightness is less than $\sim 0\farcs0012$ yr$^{-1}$. Once again the estimates are in agreement, but with larger uncertainties in Francic's catalogue, presumably reflecting the somewhat fainter state of H235. As we will show in Sec. *2.3*, the radial velocity data are mildly supportive, and in Sec. *3.3*, the derived distance is also supportive of membership in the cluster. Therefore, we conclude that membership is confirmed.

## 2. OBSERVATIONS

### *2.1 Photometry*

We began the photometric study of H235 in 1986 by observing the system with the 0.4 m telescope at the Rothney Astrophysical Observatory (RAO) equipped with the Rapid Alternate Detection System (RADS, Milone *et al.* 1982), which uses a cooled GaAs detector. The comparison star which was used for the RADS photometry was an anonymous star within the 40 arcmin radius of the chopping system. Since the differential data are unaffected by extinction to first order, mean coefficients were used to reduce the data, confined to airmass less than 2, to the Johnson–Cousins system. Because many of these data were obtained under what would be conventionally described as nonphotometric conditions, no attempt was made to provide absolute photometry for the standard star; these data have been used mainly to help phase other data.

Higher precision photoelectric $BV(RI)_c$ photometry was obtained by SJS in 1989 at Table Mountain,[4] California with a similar detector. The extinction and transformation coefficients and zero points for the reduction of the latter data are given in Table 1, determined from absolute photometry on the night of 1989 Oct. 18 UT. Landolt (1983) selected area stars were used to determine the coefficients and zero points. The airmass range is given in the third column of the extinc-

[3]The uncertainties cited throughout this paper, except where noted otherwise (as in tables of modeling results where probable errors are cited), are standard deviations (*m.s.e.s*).

[4]Operated by the Jet Propulsion Laboratory, Pasadena.

TABLE 1. Extinction and transformation coefficients.

| UT Date | N | A.M. range | $k'_V$ | $k'_{B-V}$ | $k'_{V-R}$ | $k'_{R-I}$ | $k'_{V-I}$ |
|---|---|---|---|---|---|---|---|
| Oct 19 | 35 | 1.00-1.25 | 0.146 ±.008 | 0.095 ±.012 | 0.048 ±.011 | 0.021 ±.018 | 0.069 ±.019 |
| Oct 20 | 37 | 1.03-1.66 | 0.127 ±.004 | 0.110 ±.006 | 0.037 ±.006 | 0.038 ±.011 | 0.075 ±.011 |
| Oct 24 | 63 | 1.00-1.76 | 0.142 ±.003 | 0.104 ±.005 | 0.034 ±.004 | 0.061 ±.006 | 0.096 ±.006 |
| Oct 26 | 43 | 1.00-1.74 | 0.114 ±.005 | 0.106 ±.005 | 0.032 ±.005 | 0.048 ±.007 | 0.080 ±.007 |

Transformation Coefficients and Zero Points

| mag/C.I.: | V | B-V | V-R | R-I | V-I |
|---|---|---|---|---|---|
| Coeffs.: | -.023±.005 | 0.953±.005 | 1.078±.010 | 0.940±.011 | 1.016±.005 |
| Z Pts.: | 1.001±.004 | 0.183±.004 | 0.589±.002 | 0.841±.005 | 1.454±.004 |

tion data. The variable (V) star is identified in Fig. 1, a $5' \times 6'$ CCD image taken at Mt. Laguna Observatory. The comparison star used by SJS was H225=R212. The differential magnitudes in the sense comparison-check star are shown in Table 2. The magnitude and color indices of the comparison and check stars are shown at the bottom of Table 2. The data indicate that the comparison and check stars are suitably constant within the errors of differential photometry. H225 was classified as an F5 V star by Rebeirot. The check star is H234=S307=F279=P941. The data were reduced with nightly extinction and transformation coefficients when available, and means when not.

The Table Mountain Observatory photoelectric differential magnitudes for H235 are given in Table 3. Table 3 is presented in its complete form in the AAS CD-ROM Series, volume 4, 1995.

Subsequent to the photoelectric data we obtained 41 CCD images in *BV* and *I* passbands with the 1 m telescope at Mt.

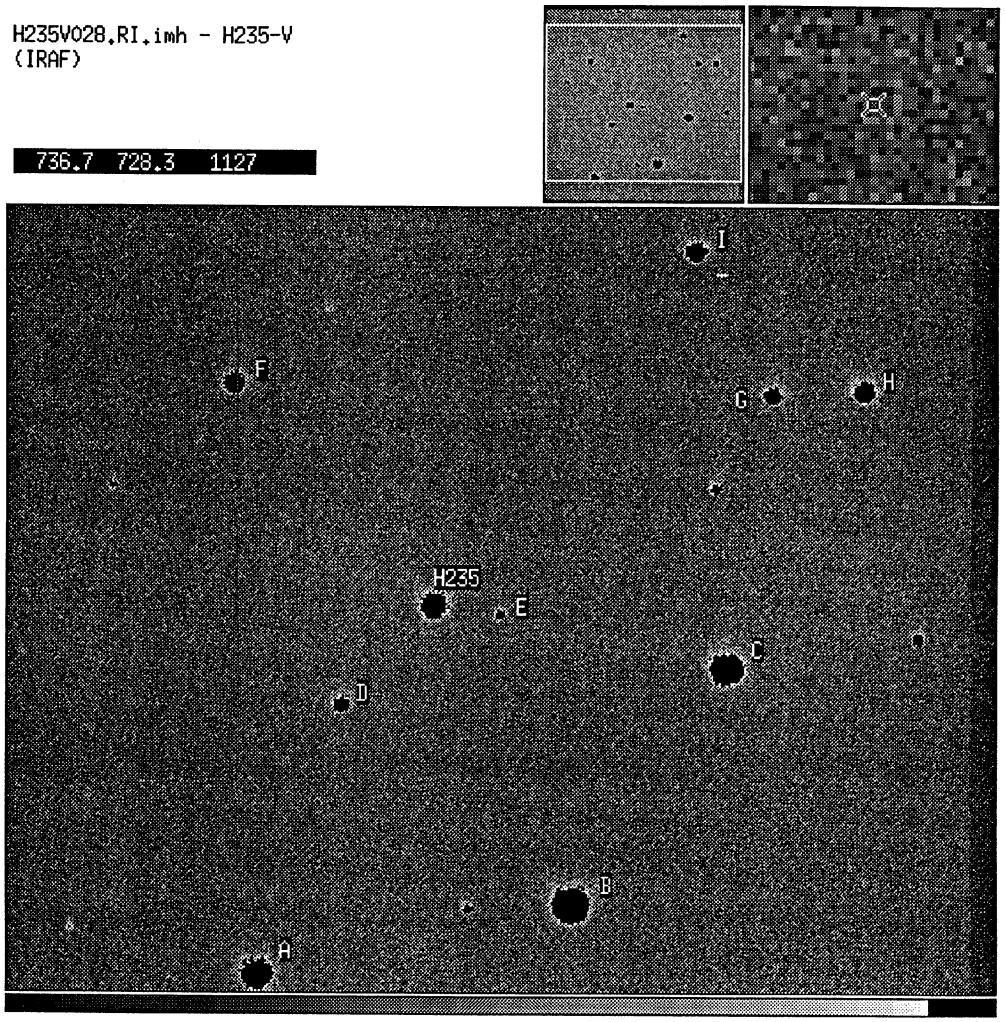


FIG. 1. A CCD image of the galactic open cluster NGC 752 showing the location of the variable H235, and comparison stars used for the CCD differential photometry.

TABLE 2. Comparison and check star magnitude and colors.

| UT Date | No. Obs. | dV | dB | dR | dI |
|---|---|---|---|---|---|
| Oct 18 | 10 | 0.522 ±.007 | 0.391 ±.011 | 0.585 ±.010 | 0.632 ±.020 |
| Oct 19 | 16 | 0.523 ±.008 | 0.400 ±.011 | 0.590 ±.010 | 0.638 ±.009 |
| Oct 20 | 14 | 0.520 ±.008 | 0.398 ±.006 | .584 ±.007 | 0.638 ±.018 |
| Oct 24 | 26 | 0.523 ±.009 | 0.400 ±.012 | 0.589 ±.008 | 0.637 ±.015 |
| Oct 26 | 16 | 0.526 ±.009 | 0.407 ±.012 | 0.585 ±.012 | 0.633 ±.017 |

**Comparison Star Means**

| Date | N | V | B-V | V-R | R-I | V-I |
|---|---|---|---|---|---|---|
| Means (Oct 18) | 17 | 10.130 ±0.007 | 0.517 ±0.009 | 0.349 ±0.010 | 0.306 ±0.015 | 0.649 ±0.018 |

**Check Star Means**

| Date | N | V | B-V | V-R | R-I | V-I |
|---|---|---|---|---|---|---|
| Means (Oct 18) | 10 | 10.654 ±0.006 | 0.386 ±0.012 | 0.287 ±0.013 | 0.248 ±0.010 | 0.528 ±0.006 |

Laguna[5] in the interval 1991 October 10–16. The Mt. Laguna CCD (Leach 1992) has the following properties: 800 ×800, 15 $\mu$m×15 $\mu$m pixels; conversion gain, 1.7 e/adu; read noise, 7 adu; and linearity to 32 000 adu. IRAF was used to reduce the images. The means of the overclocked pixels were subtracted out of each frame; after this, a median of all bias frames was obtained to determine the remaining bias structure, the subtraction of which reduced all frames to a common zero-point level. This procedure was found to produce less noise in several test frames than the subtraction of a bias structure median alone. Sky flats were used exclusively for flatfielding. Dome flats were also taken, but because some of these were taken during twilight and early daylight hours, when some possibility of daylight leakage may have contributed to the illumination of the dome screen in some frames, we decided to ignore them rather than compromise the flatfielding process. The bias-subtracted flats were medianed and then normalized and these were used to flatfield all remaining bias-subtracted frames. The IRAF task COSMICRAYS was then used to remove cosmic ray hits. The package PHOT was used to establish appropriate aperture sizes among other parameters, and aperture photometry was performed to obtain raw differential magnitudes. This operation was done frame by frame rather than automatically because seeing and hand guiding, a requirement of the system at that time, varied from frame to frame. The extinction data came from the program star frames themselves (see Fig. 1). Initially, nine stars were measured as potential comparison stars. Two of these were near bad pixels and another two were 2 mag fainter than the variable, so these data were discarded. Extinction coefficients and zero points were obtained for each star and for their mean by the linear Bouguer method. Standardization was carried out by observing selected Landolt (1983) stars in the Selected Area regions 92 and 111 at low airmasses. The extinction and transformation results for the CCD data are listed in Table 4. The CCD differential magnitudes are given in Table 5. The CCD light curve data were obtained primarily for times of minima and do not provide complete phase coverage in themselves; they are included here for future use only.

[5]Operated by San Diego State University and jointly supported by SDSU and the University of Illinois.

TABLE 3. Photoelectric light curve data.*

| HJDN | Ph(1) | Ph(3) | dV | dB | dR | dI | d(B-V) | d(V-R) | d(V-I) |
|---|---|---|---|---|---|---|---|---|---|
| 2 400 000+ | | | | | | | | | |
| 47817.9628 | 0.3735 | 0.3649 | 1.234 | 1.181 | 1.287 | 1.341 | -0.053 | -0.052 | -0.107 |
| 47817.9633 | 0.3748 | 0.3662 | 1.230 | 1.167 | 1.286 | 1.333 | -0.064 | -0.055 | -0.102 |
| 47817.9639 | 0.3761 | 0.3676 | 1.254 | 1.165 | 1.292 | 1.343 | -0.089 | -0.038 | -0.089 |
| 47817.9644 | 0.3775 | 0.3689 | 1.255 | 1.161 | 1.284 | 1.338 | -0.095 | -0.029 | -0.083 |
| 47817.9650 | 0.3788 | 0.3702 | 1.255 | 1.174 | 1.284 | 1.344 | -0.081 | -0.029 | -0.089 |
| 47817.9655 | 0.3802 | 0.3716 | 1.252 | 1.174 | 1.278 | 0.000 | -0.078 | -0.025 | ... |
| 47817.9695 | 0.3897 | 0.3811 | 1.259 | 1.195 | 1.283 | 1.329 | -0.064 | -0.024 | -0.070 |
| 47817.9700 | 0.3910 | 0.3824 | 1.251 | 1.199 | 1.301 | 1.316 | -0.052 | -0.050 | -0.065 |
| 47817.9706 | 0.3924 | 0.3838 | 1.269 | 1.198 | 1.300 | 1.343 | -0.071 | -0.031 | -0.074 |
| 47817.9711 | 0.3937 | 0.3851 | 1.268 | 1.202 | 1.305 | 1.345 | -0.066 | -0.037 | -0.077 |
| 47817.9716 | 0.3949 | 0.3864 | 1.275 | 1.194 | 1.285 | 1.366 | -0.080 | -0.010 | -0.091 |
| 47817.9722 | 0.3964 | 0.3878 | 1.268 | 1.212 | 1.287 | 1.311 | -0.055 | -0.019 | -0.044 |
| 47817.9774 | 0.4089 | 0.4004 | 1.297 | 1.221 | 1.332 | 1.276 | -0.076 | -0.034 | +0.021 |
| 47817.9780 | 0.4103 | 0.4017 | 1.296 | 1.204 | 1.314 | 1.292 | -0.091 | -0.018 | +0.004 |
| 47817.9785 | 0.4117 | 0.4031 | 1.281 | 1.217 | 1.312 | 1.300 | -0.064 | -0.031 | -0.019 |
| 47817.9791 | 0.4130 | 0.4044 | 1.290 | 1.223 | 1.328 | 1.287 | -0.067 | -0.039 | +0.003 |
| 47817.9796 | 0.4143 | 0.4058 | 1.294 | 1.216 | 1.321 | 1.268 | -0.078 | -0.027 | +0.025 |
| 47817.9802 | 0.4157 | 0.4071 | 1.285 | 1.233 | 1.323 | 1.263 | -0.051 | -0.039 | +0.021 |
| 47817.9850 | 0.4275 | 0.4189 | 1.293 | 1.258 | 1.369 | 1.319 | -0.035 | -0.076 | -0.026 |
| 47817.9856 | 0.4288 | 0.4202 | 1.294 | 1.238 | 1.349 | 1.293 | -0.056 | -0.056 | +0.001 |
| 47817.9861 | 0.4301 | 0.4215 | 1.310 | 1.230 | 1.364 | 1.313 | -0.079 | -0.055 | -0.004 |
| 47817.9867 | 0.4315 | 0.4229 | 1.317 | 1.246 | 1.359 | 1.328 | -0.072 | -0.041 | -0.010 |
| 47817.9872 | 0.4328 | 0.4242 | 1.320 | 1.249 | 1.342 | 1.323 | -0.071 | -0.022 | -0.002 |
| 47817.9878 | 0.4341 | 0.4255 | 1.334 | 1.238 | 1.367 | 1.355 | -0.096 | -0.034 | -0.022 |
| 47817.9911 | 0.4421 | 0.4335 | 1.320 | 1.263 | 1.354 | 1.357 | -0.057 | -0.034 | -0.037 |
| 47817.9916 | 0.4435 | 0.4349 | 1.333 | 1.263 | 1.368 | 1.372 | -0.070 | -0.036 | -0.039 |
| 47817.9922 | 0.4448 | 0.4362 | 1.336 | 1.280 | 1.369 | 1.400 | -0.057 | -0.033 | -0.064 |
| 47817.9927 | 0.4462 | 0.4376 | 1.342 | 1.261 | 1.378 | 1.436 | -0.082 | -0.036 | -0.094 |
| 47817.9933 | 0.4476 | 0.4390 | 1.327 | 1.267 | 1.376 | 1.382 | -0.060 | -0.049 | -0.055 |
| 47817.9938 | 0.4489 | 0.4403 | 1.335 | 1.269 | 1.355 | 1.377 | -0.066 | -0.020 | -0.042 |
| 47817.9976 | 0.4580 | 0.4494 | 1.352 | 1.290 | 1.356 | 1.406 | -0.062 | -0.004 | -0.054 |
| 47817.9982 | 0.4594 | 0.4508 | 1.332 | 1.280 | 1.376 | 1.398 | -0.053 | -0.044 | -0.066 |
| 47817.9987 | 0.4607 | 0.4521 | 1.335 | 1.279 | 1.363 | 1.385 | -0.057 | -0.028 | -0.050 |
| 47817.9992 | 0.4620 | 0.4534 | 1.361 | 1.299 | 1.387 | 1.404 | -0.062 | -0.025 | -0.042 |
| 47817.9997 | 0.4630 | 0.4545 | 1.342 | 1.278 | 1.374 | 1.395 | -0.063 | -0.032 | -0.054 |
| 47818.0003 | 0.4646 | 0.4561 | 1.341 | 1.276 | 1.362 | 1.437 | -0.065 | -0.021 | -0.096 |
| 47818.0060 | 0.4784 | 0.4699 | 1.367 | 1.268 | 1.397 | 1.398 | -0.100 | -0.030 | -0.030 |
| 47818.0066 | 0.4798 | 0.4712 | 1.356 | 1.302 | 1.370 | 1.422 | -0.054 | -0.014 | -0.065 |
| 47818.0071 | 0.4812 | 0.4726 | 1.365 | 1.289 | 1.401 | 1.415 | -0.076 | -0.036 | -0.050 |
| 47818.0077 | 0.4825 | 0.4739 | 1.360 | 1.279 | 1.398 | 1.420 | -0.081 | -0.039 | -0.060 |
| 47818.0082 | 0.4838 | 0.4753 | 1.358 | 1.282 | 1.399 | 1.402 | -0.076 | -0.041 | -0.044 |
| 47818.0088 | 0.4852 | 0.4766 | 1.352 | 1.274 | 1.401 | 1.402 | -0.078 | -0.049 | -0.050 |
| 47818.0119 | 0.4928 | 0.4842 | 1.351 | 1.281 | 1.393 | 1.404 | -0.070 | -0.041 | -0.053 |
| 47818.0125 | 0.4941 | 0.4855 | 1.355 | 1.291 | 1.389 | 1.391 | -0.064 | -0.034 | -0.036 |
| 47818.0130 | 0.4954 | 0.4869 | 1.356 | 1.273 | 1.403 | 1.391 | -0.083 | -0.047 | -0.035 |
| 47818.0136 | 0.4968 | 0.4882 | 1.351 | 1.300 | 1.407 | 1.400 | -0.051 | -0.056 | -0.049 |
| 47818.0141 | 0.4982 | 0.4896 | 1.375 | 1.272 | 1.390 | 1.423 | -0.103 | -0.014 | -0.048 |
| 47818.0147 | 0.4995 | 0.4909 | 1.352 | 1.301 | 1.388 | 1.422 | -0.050 | -0.037 | -0.071 |
| 47818.0152 | 0.5008 | 0.4922 | 1.359 | 1.272 | 1.392 | 1.429 | -0.087 | -0.033 | -0.070 |
| 47818.0158 | 0.5021 | 0.4936 | 1.352 | 1.286 | 1.404 | 1.412 | -0.065 | -0.052 | -0.060 |
| 47818.7025 | 0.1695 | 0.1611 | 1.189 | 1.132 | 1.216 | 1.223 | -0.057 | -0.027 | -0.034 |
| 47818.7030 | 0.1709 | 0.1624 | 1.187 | 1.141 | 1.237 | 1.249 | -0.046 | -0.050 | -0.061 |
| 47818.7036 | 0.1722 | 0.1637 | 1.187 | 1.127 | 1.221 | 1.245 | -0.060 | -0.034 | -0.058 |
| 47818.7041 | 0.1735 | 0.1650 | 1.181 | 1.125 | 1.224 | 1.251 | -0.056 | -0.043 | -0.069 |
| 47818.7046 | 0.1748 | 0.1663 | 1.189 | 1.125 | 1.227 | 1.243 | -0.064 | -0.038 | -0.054 |
| 47818.7052 | 0.1762 | 0.1677 | 1.186 | 1.132 | 1.217 | 1.247 | -0.054 | -0.031 | -0.061 |
| 47818.7057 | 0.1775 | 0.1690 | 1.195 | 1.146 | 1.246 | 1.269 | -0.049 | -0.050 | -0.074 |
| 47818.7063 | 0.1788 | 0.1703 | 1.187 | 1.143 | 1.221 | 1.237 | -0.044 | -0.034 | -0.050 |
| 47818.7068 | 0.1801 | 0.1717 | 1.184 | 1.120 | 1.227 | 1.238 | -0.064 | -0.044 | -0.054 |
| 47818.7074 | 0.1814 | 0.1730 | 1.189 | 1.118 | 1.238 | 1.245 | -0.070 | -0.050 | -0.056 |
| 47818.7134 | 0.1960 | 0.1875 | 1.166 | 1.098 | 1.199 | 1.230 | -0.068 | -0.033 | -0.064 |
| 47818.7139 | 0.1973 | 0.1888 | 1.157 | 1.096 | 1.197 | 1.237 | -0.061 | -0.040 | -0.080 |
| 47818.7144 | 0.1986 | 0.1902 | 1.175 | 1.089 | 1.202 | 1.225 | -0.086 | -0.027 | -0.050 |
| 47818.7150 | 0.2000 | 0.1915 | 1.163 | 1.095 | 1.187 | 1.222 | -0.069 | -0.024 | -0.059 |
| 47818.7155 | 0.2013 | 0.1928 | 1.166 | 1.101 | 1.208 | 1.230 | -0.065 | -0.042 | -0.064 |
| 47818.7161 | 0.2026 | 0.1941 | 1.169 | 1.111 | 1.203 | 1.237 | -0.057 | -0.034 | -0.068 |
| 47818.7166 | 0.2039 | 0.1954 | 1.158 | 1.118 | 1.196 | 1.240 | -0.040 | -0.038 | -0.081 |

*Table 3 is presented in its complete form in the AAS CD-ROM Series, Volume 4, 1995.

TABLE 4. CCD extinction and transformation data.

| UT Date | N | A.M. range | $k'_B$ | $k'_V$ | $k'_I$ |
|---|---|---|---|---|---|
| 1991 Oct 16 | 42,42,35 | 1.0 - 1.9 | 0.240 ±.007 | 0.190 ±.006 | 0.065 ±.009 |

**Transformation Coefficients and Zero Points**

| mag/C.I.: | V | B-V | V-I |
|---|---|---|---|
| Coeffs.: | -0.030±.017 | 1.159±.019 | 0.925±.013 |
| Z Pts.: | -10.103±.067 | -0.674±.065 | 0.680±.043 |

**Mean Comparison Star Data**

| UT Date | N | A.M. range | $<b_0>$ | $<v_0>$ | $<i_0>$ |
|---|---|---|---|---|---|
| 1991 Oct 16 | 42,42,35 | 1.0 - 1.9 | 22.829 ±0.012 | 21.873 ±0.012 | 21.976 ±0.016 |

| UT Date | <V> | <B-V> | <V-I> |
|---|---|---|---|
| 1991 Oct 16 | 12.710 ±0.027 | 0.461 ±0.027 | 0.555 ±0.016 |

At this point, only the Table Mountain data are of sufficiently high precision and completeness to permit analysis, and so these were used to carry out the light curve analyses reported here. The data were binned and averaged, a process which provided the standard deviations which were used to create weights for the light curve analysis. The binning was accomplished by averaging intensities and phases for all points in phase bins of $0^P.01$. The binned light curve data and their weights are listed in Table 6. In Sec. 4 we present the evidence for variable asymmetries in the light curves, which precludes combination of partial light curves from different epochs, at least at the present time. When a sufficient series of light curves are available to analyze the asymmetries for time-dependent effects, more use may be made of these data. The analyzed light curves are displayed in Fig. 2.

### 2.2 *Times and Phases of Minimum*

Times of minima were determined by SJS with PHIMIN (Milone *et al.* 1980), and were initially phased with his preliminary elements. Phases of minima for the RAO and Mt. Laguna data were obtained from a newer version of the PHIMIN program by J. R. McVean, called EXTREME, which gives the same results, but has graphical screen facilities to examine and discard and restore data, assist parameter selection, check progress, and examine fittings. The ephemeris was initially determined by SJS from the Table Mountain data alone to be

$$E_0 = 2\ 447\ 815.338(3), \quad P = 0.411\ 83(12)\text{d}, \qquad (1)$$

where the uncertainties (in parentheses) are in units of the last place.

Times of minima from the RAO and MLO data were determined also and the three sets of data were used to obtain a new linear ephemeris:

$$E_0 = 2\ 446\ 785.855(13), \quad P = 0.411\ 798(2)\text{d}. \qquad (2)$$

However, a better fit is obtained from the quadratic equation of condition

$$T_{\min} = a + bn + cn^2,$$

yielding the elements

$$a \equiv E_0 = 2\ 446\ 785.8660(23),$$
$$b \equiv P = 0.411\ 775\ 0(10)\text{d}, \qquad (3)$$
$$c = 6.11(25) \times 10^{-9},$$

implying that

$$q = 1.484(63) \times 10^{-8}\ \text{d/d}.$$

While a discrete period change is possible, a variable period provides a better fit to all the data. These elements still give relatively large residuals for the accurately determined TMO and MLO minima; a better fit to these minima is provided by a linear ephemeris involving only those data. These elements are

$$E_0 = 2\ 446\ 785.8003(25), \quad P = 0.411\ 816\ 5(9)\text{d}. \qquad (4)$$

The times of minima and the corresponding O−C results for each ephemeris are given in Table 7 and are illustrated in

TABLE 5. CCD light curve data.

| HJDN | Φ | dI | HJDN | Φ | dV | HJDN | Φ | dB |
|---|---|---|---|---|---|---|---|---|
| 8545.8363 | 0.7861 | -0.4037 | 8545.8415 | 0.7987 | -0.3916 | 8545.8443 | 0.8054 | -0.3981 |
| 8545.8387 | 0.7919 | -0.3999 | 8545.8430 | 0.8022 | -0.3911 | 8545.8470 | 0.8121 | -0.3887 |
| 8545.8456 | 0.8086 | -0.3830 | 8545.8463 | 0.8104 | -0.3751 | 8545.8499 | 0.8190 | -0.3687 |
| 8545.8482 | 0.8149 | -0.3604 | 8545.8490 | 0.8169 | -0.3629 | 8545.8518 | 0.8237 | -0.3683 |
| 8545.8506 | 0.8207 | -0.3533 | 8545.8511 | 0.8220 | -0.3646 | 8545.8541 | 0.8292 | -0.3601 |
| 8545.8525 | 0.8253 | -0.3521 | 8545.8531 | 0.8267 | -0.3656 | 8545.8565 | 0.8351 | -0.3551 |
| 8545.8549 | 0.8311 | -0.3477 | 8545.8558 | 0.8333 | -0.3550 | 8545.8589 | 0.8410 | -0.3461 |
| 8545.8572 | 0.8368 | -0.3424 | 8545.8578 | 0.8382 | -0.3439 | 8545.8612 | 0.8465 | -0.3410 |
| 8545.8596 | 0.8426 | -0.3307 | 8545.8602 | 0.8441 | -0.3406 | 8545.8640 | 0.8533 | -0.3271 |
| 8545.8623 | 0.8491 | -0.3110 | 8545.8630 | 0.8509 | -0.3310 | 8545.8659 | 0.8578 | -0.3286 |
| 8545.8647 | 0.8549 | -0.3193 | 8545.8656 | 0.8572 | -0.3214 | 8545.8682 | 0.8635 | -0.3169 |
| 8545.8667 | 0.8599 | -0.3086 | 8545.8673 | 0.8612 | -0.2973 | 8545.8713 | 0.8710 | -0.2930 |
| 8545.8697 | 0.8671 | -0.3004 | 8545.8704 | 0.8689 | -0.2909 | 8545.8731 | 0.8755 | -0.2876 |
| 8545.8719 | 0.8725 | -0.2947 | 8545.8725 | 0.8739 | -0.2946 | 8545.8768 | 0.8844 | -0.2811 |
| 8545.8737 | 0.8769 | -0.2927 | 8545.8744 | 0.8785 | -0.2864 | 8545.8801 | 0.8924 | -0.2783 |
| 8545.8757 | 0.8817 | -0.2861 | 8545.8762 | 0.8830 | -0.2799 | 8545.8824 | 0.8979 | -0.2703 |
| 8545.8779 | 0.8870 | -0.2776 | 8545.8788 | 0.8892 | -0.2624 | 8545.8880 | 0.9115 | -0.2470 |
| 8545.8812 | 0.8950 | -0.2731 | 8545.8817 | 0.8963 | -0.2646 | 8545.8933 | 0.9245 | -0.2407 |
| 8545.8837 | 0.9011 | -0.2584 | 8545.8927 | 0.9230 | -0.2346 | 8545.9014 | 0.9442 | -0.2283 |
| 8545.8921 | 0.9216 | -0.2364 | 8545.8990 | 0.9384 | -0.2351 | 8545.9066 | 0.9566 | -0.2249 |
| 8545.8949 | 0.9284 | -0.2339 | 8545.9050 | 0.9528 | -0.2317 | 8545.9111 | 0.9677 | -0.2343 |
| 8545.9036 | 0.9494 | -0.2253 | 8545.9102 | 0.9655 | -0.2257 | 8545.9167 | 0.9813 | -0.2394 |
| 8545.9091 | 0.9628 | -0.2359 | 8545.9159 | 0.9793 | -0.2383 | 8545.9214 | 0.9926 | -0.2547 |
| 8545.9131 | 0.9724 | -0.2334 | 8545.9203 | 0.9899 | -0.2514 | 8545.9373 | 1.0312 | -0.4363 |
| 8545.9192 | 0.9873 | -0.2469 | 8545.9359 | 1.0278 | -0.2969 | 8545.9547 | 1.0735 | -0.3513 |
| 8545.9352 | 1.0261 | -0.2853 | 8545.9394 | 1.0363 | -0.3019 | 8545.9750 | 1.1229 | -0.4639 |
| 8545.9384 | 1.0340 | -0.3013 | 8545.9437 | 1.0468 | -0.3181 | 8545.9808 | 1.1369 | -0.4244 |
| 8545.9424 | 1.0436 | -0.3097 | 8545.9536 | 1.0709 | -0.3489 | 8546.0017 | 1.1877 | -0.4571 |
| 8545.9528 | 1.0690 | -0.3400 | 8545.9563 | 1.0775 | -0.3593 | 8546.0048 | 1.1952 | -0.4534 |
| 8545.9556 | 1.0758 | -0.3460 | 8545.9740 | 1.1205 | -0.4117 | 8546.0173 | 1.2256 | -0.4501 |
| 8545.9730 | 1.1180 | -0.3977 | 8545.9788 | 1.1320 | -0.4151 | 8546.0300 | 1.2565 | -0.4241 |
| 8545.9771 | 1.1278 | -0.4061 | 8546.0007 | 1.1852 | -0.4501 | 8546.0330 | 1.2637 | -0.4180 |
| 8545.9995 | 1.1824 | -0.4281 | 8546.0038 | 1.1927 | -0.4471 | 8546.0359 | 1.2706 | -0.4149 |
| 8546.0028 | 1.1904 | -0.4391 | 8546.0163 | 1.2231 | -0.4457 | 8546.0413 | 1.2839 | -0.3953 |
| 8546.0143 | 1.2182 | -0.4227 | 8546.0192 | 1.2302 | -0.4337 | 8546.0461 | 1.2956 | -0.3780 |
| 8546.0184 | 1.2281 | -0.4321 | 8546.0257 | 1.2460 | -0.4339 | 8546.0494 | 1.3035 | -0.3553 |
| 8546.0245 | 1.2431 | -0.4307 | 8546.0287 | 1.2533 | -0.4250 | | | |
| 8546.0277 | 1.2508 | -0.4203 | 8546.0320 | 1.2613 | -0.4206 | | | |
| 8546.0311 | 1.2589 | -0.4281 | 8546.0349 | 1.2682 | -0.4119 | | | |
| 8546.0341 | 1.2663 | -0.4077 | 8546.0401 | 1.2808 | -0.4046 | | | |
| 8546.0370 | 1.2733 | -0.4007 | 8546.0452 | 1.2933 | -0.3957 | | | |
| 8546.0437 | 1.2896 | -0.3946 | 8546.0484 | 1.3009 | -0.3544 | | | |
| 8546.0475 | 1.2988 | -0.3341 | | | | | | |

TABLE 6. Binned photometric input data.

| Passband ($\lambda_0$) Φ v/l w | Φ v/l w | Φ v/l w | Φ v/l w | Φ v/l w |
|---|---|---|---|---|
| B (0.44): | | | | |
| .00490.7954 07 | .01290.8015 05 | .02670.8067 11 | .03310.8073 04 | .04600.8153 08 |
| .05850.8281 02 | .06460.8330 07 | .07040.8354 01 | .08670.8605 06 | .09330.8658 04 |
| .10600.8818 04 | .11330.8862 05 | .13000.9043 01 | .13330.9001 04 | .15540.9320 05 |
| .16800.9363 04 | .17480.9309 00 | .18350.9483 00 | .19800.9598 10 | .20420.9609 00 |
| .21440.9722 13 | .22450.9729 11 | .23420.9771 10 | .24570.9792 10 | .25130.9794 04 |
| .26690.9830 02 | .27420.9773 07 | .28740.9836 03 | .29510.9685 11 | .30360.9666 07 |
| .31650.9485 09 | .32550.9538 13 | .33390.9398 09 | .34600.9318 17 | .35310.9167 06 |
| .36550.9147 07 | .37580.8983 17 | .38490.8887 09 | .39300.8742 09 | .40620.8684 13 |
| .41370.8600 16 | .42570.8453 11 | .43430.8393 12 | .44510.8256 21 | .45490.8157 13 |
| .46430.8118 17 | .47690.8030 14 | .48400.8018 21 | .49510.8049 16 | .50470.8024 09 |
| .51590.8059 13 | .52520.8070 15 | .53470.8097 11 | .54560.8145 11 | .55500.8181 21 |
| .56380.8335 16 | .57520.8312 00 | .58490.8497 14 | .59500.8675 16 | .60450.8841 08 |
| .61620.8771 05 | .62470.9019 08 | .63530.9186 08 | .64370.9244 05 | .65830.9376 05 |
| .66490.9417 15 | .67480.9483 15 | .68340.9455 10 | .69670.9697 13 | .70490.9726 18 |
| .71480.9810 14 | .72910.9816 03 | .73440.9835 09 | .74460.9850 09 | .75290.9895 04 |
| .76840.9773 03 | .77490.9749 14 | .78400.9739 11 | .79560.9677 06 | .80560.9621 15 |
| .81490.9604 06 | .82390.9480 05 | .84790.9252 03 | .85600.9213 12 | .86490.9165 13 |
| .87100.8996 02 | .88490.8922 10 | .89300.8757 04 | .90880.8680 01 | .91560.8636 07 |
| .92220.8609 03 | .93710.8260 05 | .96690.8231 04 | .97020.8140 01 | .98300.8042 06 |
| .99830.8048 03 | | | | |
| V (0.55): | | | | |
| .00490.8032 07 | .02670.8153 11 | .03310.8161 04 | .04600.8325 08 | .05850.8334 02 |
| .06460.8436 07 | .07040.8501 01 | .08670.8664 06 | .09330.8708 04 | .10600.8807 04 |
| .11330.8923 05 | .13000.9100 01 | .13330.9178 04 | .15540.9381 05 | .16800.9439 04 |
| .17480.9468 11 | .18350.9510 00 | .19800.9673 10 | .20420.9726 15 | .21420.9805 11 |
| .22450.9785 11 | .23420.9839 10 | .24570.9835 10 | .25130.9865 04 | .26690.9954 02 |
| .27420.9908 07 | .28740.9855 03 | .29510.9735 11 | .30360.9707 07 | .31650.9691 09 |
| .32550.9621 13 | .33390.9545 09 | .34600.9429 17 | .35310.9364 06 | .36550.9104 07 |
| .37580.9056 17 | .38490.8968 09 | .39300.8863 09 | .40620.8764 13 | .41370.8703 16 |
| .42570.8571 11 | .43430.8481 12 | .44510.8384 21 | .45490.8315 13 | .46430.8263 17 |
| .47690.8137 14 | .48400.8104 21 | .49510.8114 16 | .50470.8074 09 | .51590.8120 13 |
| .52520.8171 15 | .53470.8162 11 | .54560.8248 11 | .55500.8296 21 | .56380.8433 16 |
| .57520.8482 14 | .58490.8660 14 | .59500.8798 16 | .60450.8911 08 | .61620.8917 05 |
| .62470.9097 08 | .63530.9277 08 | .64370.9374 05 | .65830.9403 05 | .66490.9491 15 |
| .67480.9529 15 | .68340.9539 10 | .69670.9770 13 | .70490.9792 18 | .71480.9879 14 |
| .72910.9937 03 | .73440.9924 09 | .74460.9903 09 | .75290.9852 04 | .76840.9803 03 |
| V (0.55), continued | | | | |
| .77490.9845 14 | .78400.9841 11 | .79560.9838 06 | .80560.9734 15 | .81490.9670 06 |
| .82390.9567 05 | .84790.9297 03 | .85600.9299 12 | .86490.9236 13 | .87100.9065 02 |
| .88490.9074 10 | .89300.8932 04 | .90880.8686 01 | .91560.8764 07 | .92220.8636 03 |
| .93710.8434 05 | .96690.8244 04 | .97020.8262 01 | .98300.8110 06 | .99830.8110 03 |

| Passband ($\lambda_0$) Φ v/l w | Φ v/l w | Φ v/l w | Φ v/l w | Φ v/l w |
|---|---|---|---|---|
| Rc (.64): | | | | |
| .00490.7986 07 | .01290.8347 00 | .02670.8072 11 | .03310.8105 04 | .04600.8220 08 |
| .05850.8405 02 | .06460.8390 07 | .07040.8539 01 | .08630.8549 05 | .09330.8660 04 |
| .10600.8746 04 | .11330.8825 05 | .13000.8884 01 | .13330.9026 04 | .15540.9214 05 |
| .16800.9311 04 | .17480.9311 11 | .18350.9401 09 | .19800.9510 10 | .20420.9564 15 |
| .21440.9701 13 | .22450.9630 11 | .23420.9716 10 | .24570.9702 10 | .25130.9758 04 |
| .26690.9639 02 | .27420.9635 07 | .28740.9607 03 | .29510.9618 11 | .30360.9427 07 |
| .31650.9529 09 | .32550.9485 13 | .33390.9420 09 | .34600.9333 17 | .35310.9200 06 |
| .36550.9021 07 | .37580.8928 17 | .38490.8881 09 | .39300.8814 09 | .40620.8704 13 |
| .41370.8597 16 | .42570.8416 11 | .43430.8319 12 | .44510.8257 21 | .45490.8215 13 |
| .46440.8165 16 | .47690.8044 14 | .48410.7989 20 | .49510.7987 16 | .50470.7914 09 |
| .51590.8023 13 | .52520.8094 15 | .53470.8114 11 | .54560.8142 11 | .55500.8217 21 |
| .56380.8341 16 | .57520.8424 14 | .58490.8539 14 | .59500.8671 16 | .60450.8790 08 |
| .61620.8758 05 | .62470.8981 08 | .63530.9141 08 | .64370.9228 05 | .65830.9261 05 |
| .66510.9421 14 | .67480.9462 15 | .68340.9525 10 | .69670.9667 00 | .70490.9655 18 |
| .71480.9738 14 | .72910.9775 03 | .73440.9750 09 | .74460.9732 09 | .75290.9724 04 |
| .76840.9642 03 | .77490.9713 14 | .78400.9656 11 | .79560.9688 06 | .80560.9574 15 |
| .81490.9559 06 | .82390.9495 05 | .84790.9122 03 | .85600.9190 12 | .86490.9142 13 |
| .87100.8912 02 | .88490.8923 10 | .89300.8886 04 | .90880.8264 01 | .91560.8613 07 |
| .92220.8503 03 | .93710.8360 05 | .96690.8235 04 | .97020.8067 01 | .98300.8015 06 |
| .99830.7944 03 | | | | |
| Ic (.82) | | | | |
| .00490.7867 07 | .01290.8073 05 | .02670.7984 11 | .03310.7968 04 | .04600.8102 08 |
| .05850.8297 02 | .06460.8340 07 | .07040.8293 01 | .08670.8441 06 | .09330.8423 04 |
| .10600.8692 04 | .11330.9044 05 | .13000.9095 01 | .13330.9143 04 | .15540.8975 05 |
| .16800.9439 04 | .17520.9210 10 | .18350.9247 09 | .19800.9386 10 | .20420.9392 15 |
| .21420.9493 11 | .22450.9508 11 | .23420.9517 10 | .24570.9503 10 | .25130.9530 04 |
| .26690.9499 02 | .27420.9495 07 | .28740.9497 03 | .29510.9361 11 | .30360.9374 07 |
| .31650.9347 09 | .32550.9298 13 | .33390.9264 09 | .34600.9180 17 | .35310.9108 06 |
| .36550.8913 07 | .37580.8703 17 | .38550.8724 08 | .39300.8548 09 | .40620.8576 13 |
| .41370.8607 16 | .42570.8423 11 | .43430.8354 12 | .44510.8147 21 | .45490.8087 13 |
| .46430.7979 17 | .47690.7880 14 | .48400.7895 21 | .49510.7919 16 | .50470.7855 09 |
| Ic (0.82), continued | | | | |
| .51590.7915 13 | .52520.7953 15 | .53470.7965 11 | .54560.8093 11 | .55500.8116 21 |
| .56380.8227 16 | .57540.8315 07 | .58570.8475 11 | .59500.8572 16 | .60450.8669 08 |
| .61620.8641 05 | .62470.8900 08 | .63530.9065 08 | .64370.9102 05 | .65830.9130 05 |
| .66490.9368 15 | .67480.9481 00 | .68340.9546 10 | .69670.9637 00 | .70490.9573 18 |
| .71480.9644 14 | .72910.9757 03 | .73440.9578 09 | .74460.9605 09 | .75290.9468 04 |
| .76840.9494 03 | .77490.9487 14 | .78400.9437 11 | .79560.9505 06 | .80560.9462 15 |
| .81490.9514 06 | .82390.9616 05 | .84790.9269 03 | .85600.9255 12 | .86490.9144 13 |
| .87100.8943 02 | .88490.8751 10 | .89300.8379 04 | .90880.7941 01 | .91560.8525 07 |
| .92220.8351 03 | .93710.7861 00 | .96690.7995 04 | .97020.7929 01 | .98300.7972 06 |
| .99830.7872 03 | | | | |

Fig. 3. $(O-C)_1$ are the residuals from ephemeris (1), $(O-C)_2$ are those from ephemeris (2), etc., all expressed in units of phase. However, an examination of the data phased with each of the ephemerides, shows that the best apparent fit to the TMO minima alone is that given by ephemeris (1). This suggests that a period change may have taken place between 1986 and 1987, either on top of a continual change or with another discrete change at a later epoch. Therefore, the true behavior of the O−C curves is insufficiently described by either quadratic or linear ephemerides and so, in the absence of definitive results from the O−C analyses, ephemeris (1) was used for the phases of Table 3 and elsewhere and for the analyses of the light curves shown in Fig. 2. Table 3 also includes phases computed with ephemeris (3) as an aid to future modeling. To insure that the lack of proper phasing did not compromise the light curve modeling process, the phase shift parameter, $\Delta\phi$, was adjusted and optimized, as noted below. The light curve extrema for critical phases are listed in Table 8. The radial velocity data were phased separately as we note below.

### *2.3 Spectroscopy*

Ebbighausen (1939) assigned H235 a spectral class of F6, while Roman (1955) and Rebeirot (1970) assigned it a spectral class of F5. Our assessment of the spectral type is F3–5, based on the relative strengths of the hydrogen and metal lines. The relative strengths of the *G* band, λ4325, and Hγ make it appear earlier than the F7 dwarf HD114762 and slightly later, but certainly very close to, the spectral type of HD 181096 (dF3 according to the compilation of Abt & Biggs 1972). The present spectroscopy was carried out at DAO mostly in the interval 1985 to 1987. The bulk of our data is in the form of exposures of an intensified Reticon linear array detector with 1892 elements at the output of the 21121 spectrograph on the 1.8 m telescope. The nominal dispersion of the spectrograph is 15 Å/mm. The data were reduced using the REDUCE and VCROSS software of G. Hill (Hill 1982). The spectra were cross correlated against three standard stars. The cross-correlation functions (hereafter designated CCFs), illustrated in Fig. 4, are noisy, but usable, and the phase coverage was not uniform due to an incorrect epoch in the ephemeris used for observational planning. Subsequently, the intensified reticon was retired because the image intensifier required an umbilicus to carry dry, cool nitrogen gas to the intensifier dynodes, and this limited telescope mobility. Subsequent unintensified CCD exposures obtained with the same spectrograph have not proved as well suited to study this low-S/N, high light-ratio, and strongly phase-limited object. Hopefully, improved detectors will be available in the future, so that features can be better resolved and measured at lower dispersion.

The reticon exposures were reduced with Hill's REDUCE

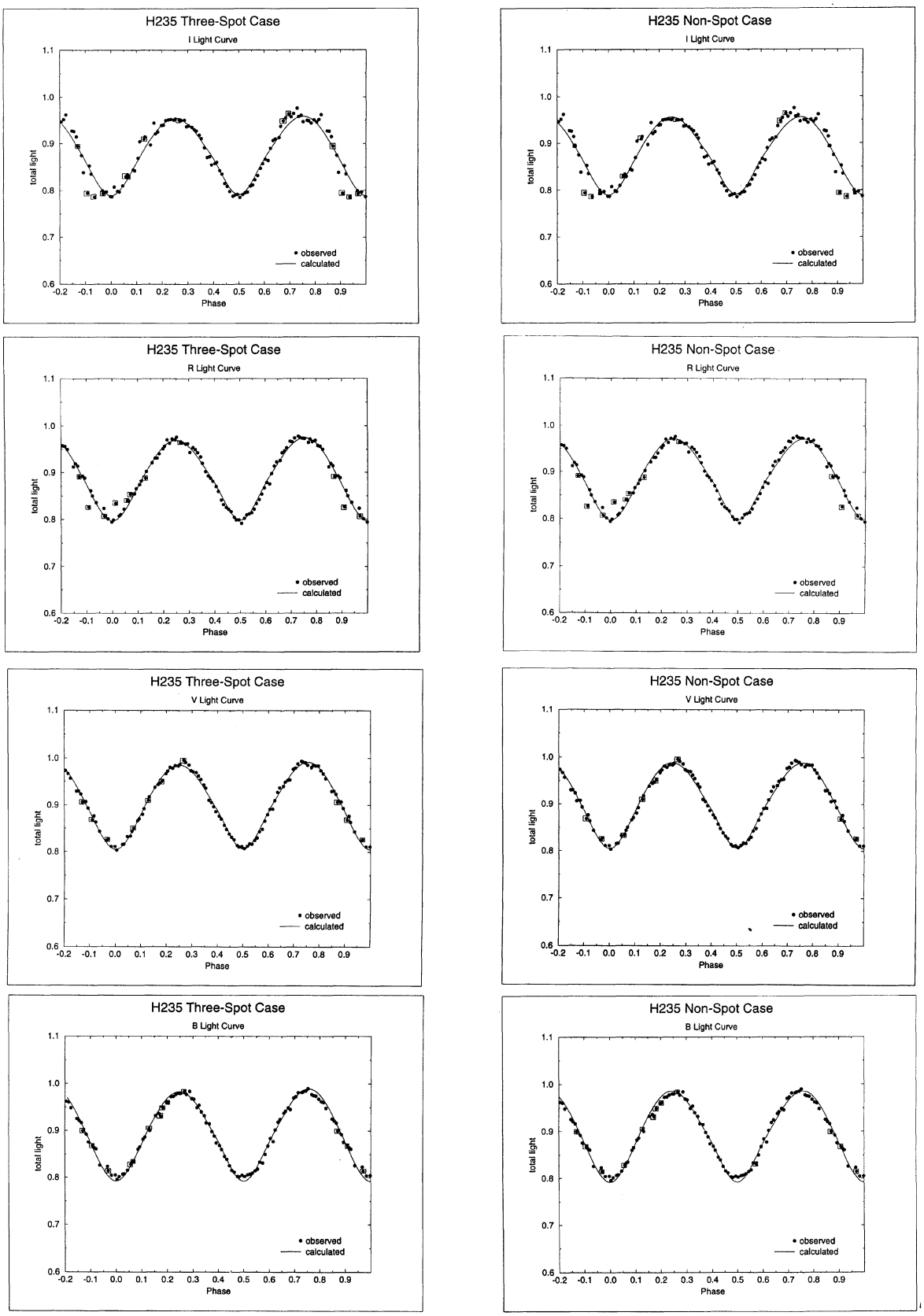


FIG. 2. Observed and computed $BV(RI)_C$ light curves of the system H235 for the best spot and nonspot models. The observed data are binned normals, as discussed in the text. The squares mark data points of low or zero weight.

TABLE 7. Times of minimum.

| Data | HJDN - 2400000 | λ | M | $(O-C)_1$ | $(O-C)_2$ | $(O-C)_3$ | $(O-C)_4$ |
|---|---|---|---|---|---|---|---|
| RAO | 46795.74854(4) | I | P | +0.24675 | +0.02465 | -0.00025 | (+0.06485) |
| RAO | 46795.74723(3) | R | P | +0.24357 | +0.02147 | -0.00343 | (+0.06337) |
| RAO | 46795.75102(2) | V | P | +0.25277 | +0.03068 | +0.00577 | (+0.06717) |
| RAO | 46795.74749(3) | B | P | +0.24420 | +0.02210 | -0.00280 | (+0.06364) |
| RAO | 46795.74893(8) | U | P | +0.24770 | +0.02560 | +0.00070 | (+0.06508) |
| TMO | 47818.84173(6) | I | S | +0.00771 | -0.02129 | -0.00101 | -0.00031 |
| TMO | 47818.84174(6) | R | S | +0.00772 | -0.02127 | -0.00099 | -0.00030 |
| TMO | 47818.84173(8) | V | S | +0.00771 | -0.02129 | -0.00101 | -0.00031 |
| TMO | 47818.84174(6) | B | S | +0.00772 | -0.02127 | -0.00099 | -0.00030 |
| TMO | 47823.78056(6) | I | S | +0.00011 | -0.02795 | -0.00790 | -0.00327 |
| TMO | 47823.78056(6) | R | S | +0.00012 | -0.02795 | -0.00789 | -0.00327 |
| TMO | 47823.78056(8) | V | S | +0.00011 | -0.02796 | -0.00791 | -0.00328 |
| TMO | 47823.78059(6) | B | S | +0.00018 | -0.02788 | -0.00783 | -0.00325 |
| TMO | 47823.99351(11) | I | P | +0.01718 | -0.01084 | +0.00921 | +0.00376 |
| TMO | 47823.99351(11) | I | P | +0.01718 | -0.01084 | +0.00921 | +0.00376 |
| TMO | 47823.99348(14) | R | P | +0.01713 | -0.01090 | +0.00915 | +0.00374 |
| TMO | 47823.99350(9) | V | P | +0.01716 | -0.01087 | +0.00918 | +0.00375 |
| TMO | 47823.99351(11) | I | P | +0.01718 | -0.01084 | +0.00921 | +0.00376 |
| TMO | 47823.99348(14) | R | P | +0.01713 | -0.01090 | +0.00915 | +0.00374 |
| TMO | 47823.99350(9) | V | P | +0.01716 | -0.01087 | +0.00918 | +0.00375 |
| TMO | 47823.99351(3) | B | P | +0.01719 | -0.01083 | +0.00921 | +0.00377 |
| TMO | 47825.84266(19) | I | S | +0.00733 | -0.02040 | -0.00044 | -0.00026 |
| TMO | 47825.84268(21) | V | S | +0.00733 | -0.02044 | -0.00039 | -0.00023 |
| TMO | 47825.84269(17) | B | S | +0.00734 | -0.02034 | -0.00038 | -0.00023 |

software package and radial velocities were obtained with his VCROSS cross-correlation package. The comparison stars which were used for the CCFs are listed in Table 9, along with their adopted means. The averages with respect to the spectra of HD 154417 showed the least scatter, and essentially, it was used to determine the relative velocities, and the CCF results from the other stars being used essentially in a confirmatory role. The average radial velocities are shown in Table 10 and in Fig. 5. The gamma velocity of the system was determined from the light- and radial velocity curve modeling. From the radial velocity data analyzed alone, $V_\gamma = 11 \pm 2$ km s$^{-1}$, while in combination with the photometric data, the optimum value was found to be $17 \pm 4$ km s$^{-1}$, in both cases constrained to be identical for both components. The values are somewhat large compared to published mean values of the cluster: $+6.9 \pm 2.0$ (Friel & Janes 1993; 9 stars), $-4.4 \pm 2.5$ (Roman 1955), +9 (Rebeirot 1970), +5 (Pilachowski *et al.* 1986), and $+5.5 \pm 0.5$ km s$^{-1}$ (Daniel *et al.* 1994; 33 stars); but Rebeirot considered stars with velocities within $\pm 10$ km s$^{-1}$ of his value to be members. By this criterion, $V_\gamma = +12 \pm 2$ km s$^{-1}$ can be considered as mildly supportive of membership, although it is discrepant from the best precise mean of Daniel *et al.* (1994) by $2\sigma$. As we will show in later sections, the distance determined in the present analysis indicates that the system is certainly in the cluster.

## 3. LIGHT AND VELOCITY CURVE MODELING

### 3.1 Procedures

Unlike the light curves of DS And, those of H235 show the continuous variation characteristic of a tidally distorted system, which, with the system's short period, strongly suggests a contact configuration.

The modeling was carried out on a Myrias SPS-2 64-processor computer and on IBM RS6000 workstations and compute servers at the University of Calgary.

At the beginning of the modeling, we had not yet implemented the addition of the Kurucz (1993) atmospheres into the Wilson–Devinney code, and used the older version which makes use of the Kurucz (1979) atmosphere models. All stages of this upgrade have now been achieved (details and availability will be discussed by Stagg *et al.* 1995) and all final results discussed here have been achieved with the fully modernized program, which we refer to as WD93K93. It is important to note, however, that on identical data sets and with the same assumptions, the modeling results for H235 obtained with WD83K83 and WD83K93 were not significantly different. Moreover, the exploration of parameter space to insure model uniqueness and robustness has been tested with a fully upgraded version (LC93KS) of the simplex program described by Kallrath (1993), LC83KS. Simplex was first used for light curve analyses of eclipsing binary stars by Kallrath (1987) and by Kallrath & Linnell (1987). Earlier variants of the program were used by several workers (Breinhorst *et al.* 1989; Dreschel *et al.* 1989; Walker & Chambliss 1990); LC83KS was used to model the binaries in NGC 5466 (Kallrath *et al.* 1992), to check solution uniqueness in the AI Phe model (Milone *et al.* 1992) and in the model of TY Boo (Milone *et al.* 1991).

We typically run the noniterating DC routine prior to running SIMPLEX to test the preliminary model and the data for consistency. We also run DC *after* SIMPLEX to derive probable errors of the final SIMPLEX parameters. In this, as in previous studies (e.g., Kallrath *et al.* 1992) the SIMPLEX-enhanced program was used as a probe for exploring wider ranges in parameter space than is usually possible under the WD program. It provides a shortcut from initial parameters to the most likely minimum of parameter space.

For the DC runs, the general weighting constant *noise* was set equal to 1, but trials setting *noise*=0 showed no discernible differences. Radial velocity data were given uniform weight. The same weighting schemes were applied for the simplex runs. The radial velocity and data used in the analyses are listed in Table 11.

The method of multiple (and uncorrelated) subsets (Wilson & Biermann 1976) was applied for all adjustments. As is usual, however, the final errors are from the full set. All modeling was carried out in mode 3 of the WD code, appropriate for a W UMa system.

### 3.2 Initial Settings

Early in the modeling process, a transcription error in the epoch determined from the TMO photometry prevented the correct phasing of the spectroscopic data to the photometry-derived ephemeris. However, by varying the radial velocity curve phase so as to make the conjunctions coincide with either photometric minimum, we explored both W-type and A-type solutions. In each of these two solutions the sizes of the stars were comparable, the luminosity differences deriving mainly from the temperature difference between components (Milone *et al.* 1992). When the transcription error was

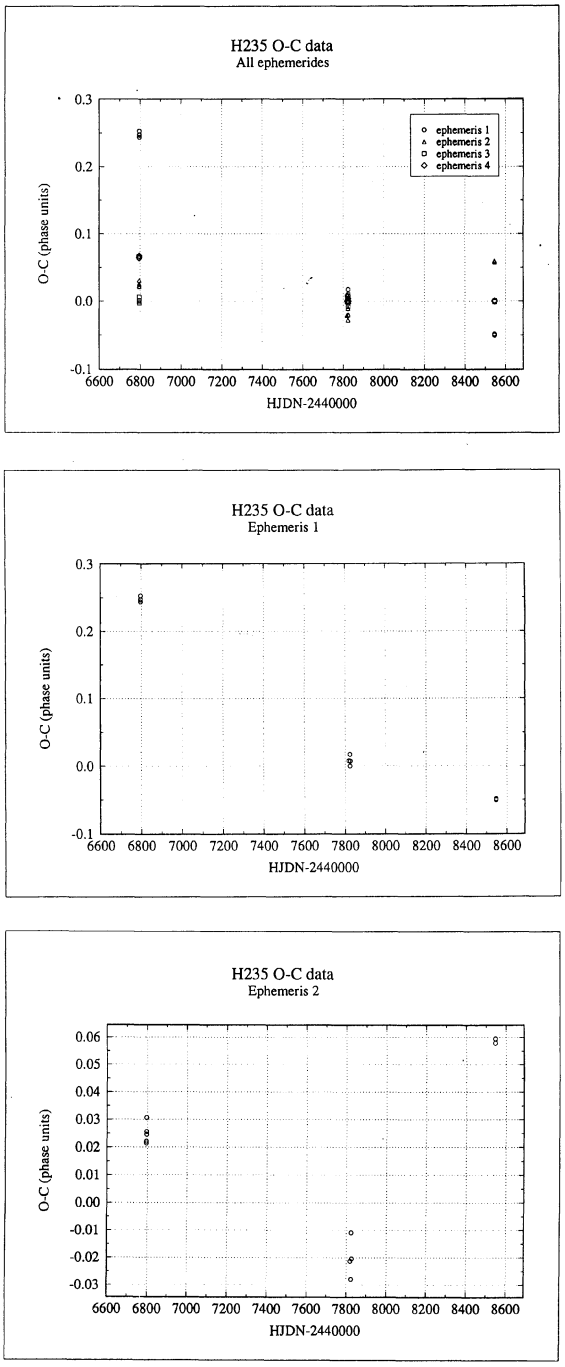


FIG. 3. Observed minus computed phases found with the software package EXTREMUM. The $(O-C)_{1,2,3,4}$ fittings refer to ephemerides (1)–(4) in the text.

discovered and the correct RV phasing approximated, the W-type solution was eliminated because the less massive star is seen to *approach* the observer prior to primary minimum and is thus the cooler of the two components.

The temperature of the primary component was assumed to be 6500 K based on the color index and the spectral type of the system. The small difference between the depths of minima dictates a similar temperature for the secondary component. The parameters which were permitted to vary were: the semimajor axis, $a$; the phase adjustment (to be added to calculated phases to match the observed light curves), $\Delta\phi$; the systemic radial velocity, $V_\gamma$; the orbital inclination to the plane of the sky, $i$; the temperature of star 2 (eclipsed at secondary minimum), $T_2$; the potential of the hotter star (assumed to be equal to that of the cooler component in a contact system), $\Omega_1$; the mass ratio, $q \equiv m_2/m_1$; and the luminosities of the hotter component, $L_1$ in the Johnson–Cousins passbands, $BV(RI)_c$. Contact, detached, and semidetached solutions were explored. The atmospheres were assumed to be radiative and so the gravity and bolometric albedos for this early F system were set equal to 1.0 for each component. The bolometric limb-darkening coefficients, needed for the the WD93K93 program, were set equal to 0.478 and 0.487 for components 1 and 2, respectively, as

TABLE 8. Light curve elements of H235.

Differential Photometry

| Extremum | dV | d(B-V) | d(V-R) | d(V-I) |
|---|---|---|---|---|
| PM | 1.361 ±.002 | -0.072 ±.002 | -0.028 ±.004 | -0.049 ±.003 |
| SM | 1.362 ±.002 | -0.072 ±.002 | -0.036 ±.002 | -0.052 ±.002 |
| max I | 1.148 ±.001 | -0.071 ±.002 | -0.032 ±.002 | -0.061 ±.002 |
| max II | 1.145 ±.001 | -0.074 ±.001 | -0.033 ±.002 | -0.062 ±.003 |

Absolute Photometry

| Extremum | V | (B-V) | (V-R) | (V-I) |
|---|---|---|---|---|
| PM | 11.491 ±.007 | +0.445 ±.009 | +0.321 ±.011 | +0.600 ±.018 |
| SM | 11.492 ±.007 | 0.445 ±.009 | 0.313 ±.010 | 0.597 ±.018 |
| max I | 11.278 ±.007 | 0.446 ±.009 | 0.317 ±.010 | 0.588 ±.018 |
| max II | 11.275 ±.007 | 0.443 ±.009 | 0.316 ±.010 | 0.587 ±.018 |

per the tables of Van Hamme (1993a, b). The passband limb-darkening coefficients were initially taken from Wade & Rucinski (1985), but later from Van Hamme (1993), which, as our referee indicated, are more consistent with our atmosphere modeling, which is also based on Kurucz's recent atmosphere models. Table 12 lists the limb-darkening coefficients and other unadjusted quantities used in the modeling trials.

The mass ratio used for the early trials, 0.155, was obtained from a preliminary analysis of the radial velocity curve of the system, but the phases of the data were not completely determined at that time and several data were

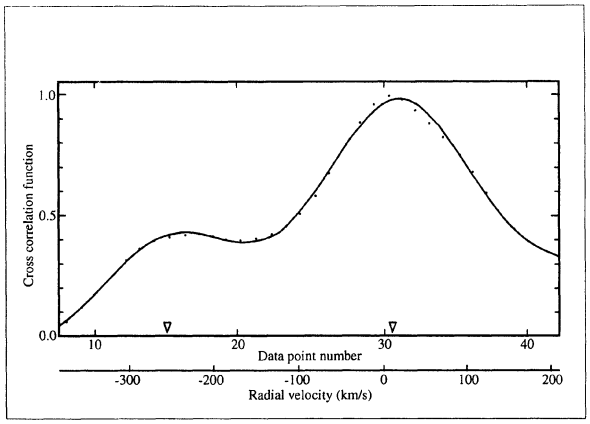


FIG. 4. Gaussian fittings to the double-peaked cross-correlation function of reticon image 2755 of H235, at phase 0.788, compared to image 2384 of the standard star HD 154417. The fitting was carried out with the use of Hill's (1982) VCROSS package.

TABLE 9. Radial velocity comparison stars.

| Star | Plate | $V_{std}$ |
|---|---|---|
| HD 154417 (G0) | S72862214, 2216 S72872384 | -17.4 ± 0.3 |
| HD 181096, (F3) | S72862184, S72872577, 2645 | +44.8 ± 0.2 |
| HD 22484, (F8) | S72872420 | +27.9 ± 0.1 |

attributed to the wrong component. With this mass ratio, and modeling the radial velocity and light curves together, convergent models were achieved for none, one, two, and three spot cases. However, at the suggestion of our referee, who made an independent analysis of our radial velocity data, we reperformed the analysis of the final set of radial velocity alone. In this run, we permitted $a$, $\Delta\phi$, $V_\gamma$, and $q$ to vary to convergence, with the value of $\sin i$ assumed from preliminary modeling of the photometric data. We then modeled the photometric data alone with the latter two values fixed, and determined a new, photometric $\Delta\phi$. The difference between the photometric and spectroscopic $\Delta\phi$ values thus repre-

TABLE 10. Radial velocity observations.

| Plate | HJDN | Phase | Exp. (sec) | $V_1$ (Km·s$^{-1}$) | $V_2$ (Km·s$^{-1}$) |
|---|---|---|---|---|---|
| 2131 | 46649.9624 | 0.9550 | 09 | + 86.9 (43) | - 44.7 (30) |
| 2187 | 46650.9131 | 0.2638 | 08 | - 57.9 (261) | +218.1 (18) |
| 2247 | 46651.9264 | 0.7246 | 06 | + 84.4 (10) | -176.0 (17) |
| 2249 | 46651.9357 | 0.7472 | 10 | +104.4 (33) | -159.6 (33) |
| 2399 | 47041.8243 | 0.7646 | 28 | + 69.6 (15) | -221.1 (33) |
| 2401 | 47041.8368 | 0.7949 | 21 | + 75.0 (30) | -201.2 (66) |
| 2403 | 47041.8535 | 0.8355 | 18 | + 64.2 (16) | -189.6 (31) |
| 2406 | 47041.8680 | 0.8707 | 15 | +103.2 (24) | - 16.8 (75) |
| 2409 | 47041.8924 | 0.9299 | 13 | + 54.8 (43) | - 77.3 (35) |
| 2411 | 47041.9070 | 0.9654 | 22 | + 49.1 (11) | ... |
| 2413 | 47041.9450 | 0.0576 | 20 | ... | + 37.7 (30) |
| 2415 | 47041.9466 | 0.0615 | 20 | - 94.3 (29): | + 59.9 (31) |
| 2417 | 47041.9466 | 0.0615 | 15 | - 26.0 (38) | +138 (179): |
| 2423 | 47042.0091 | 0.2133 | 17 | - 18.5 (11) | +200.8 (18) |
| 2425 | 47042.0236 | 0.2485 | 18 | + 30.5 (12) | +179.9 (63) |
| 2680 | 47043.9960 | 0.0386 | 14 | ... | + 23.4 (12) |
| 2682 | 47044.0043 | 0.0580 | 12 | ... | + 8.6 (10): |
| 2735 | 47045.8580 | 0.5591 | 18 | + 36.5 (62) | ... |
| 2737 | 47045.8711 | 0.5909 | 12 | + 42.2 (50) | ... |
| 2739 | 47045.8815 | 0.6162 | 12 | + 7.6 (31) | -129.1 (51) |
| 2741 | 47045.8919 | 0.6415 | 10 | + 42.4 (19) | -199.2 (68) |
| 2743 | 47045.9017 | 0.6653 | 10 | + 50.0 (23) | -187.9 (56) |
| 2745 | 47045.9121 | 0.6905 | 12 | + 42.9 (17) | -229.1 (65) |
| 2747 | 47045.9219 | 0.7143 | 09 | + 47.3 (59) | -214.2 (78) |
| 2749 | 47045.9301 | 0.7342 | 07 | + 60.5 (23) | -189.4 (69) |
| 2751 | 47045.9371 | 0.7512 | 08 | + 62.2 (18) | -225.8 (32) |
| 2753 | 47045.9448 | 0.7699 | 08 | + 77.5 (14) | -208.6 (31) |
| 2755 | 47045.9524 | 0.7884 | 08 | + 41.0 (12) | -225.4 (31) |
| 2768 | 47046.0142 | 0.9384 | 11 | ... | - 7.5 (20): |
| 2770 | 47046.0253 | 0.9654 | 11 | + 15.7 (18): | ... |
| 2772 | 47046.0336 | 0.9855 | 07 | + 24.6 (17): | ... |
| 2774 | 47046.0399 | 0.0008 | 05 | ... | + 23.6 (16): |

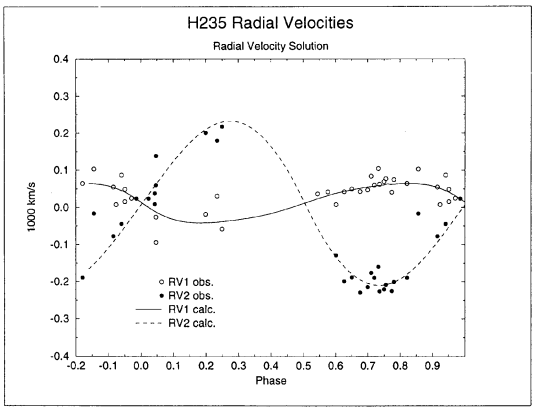


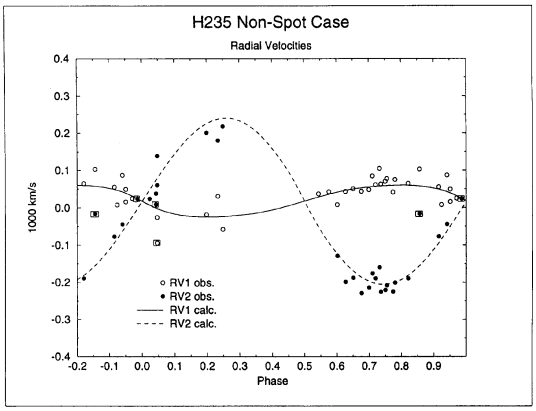


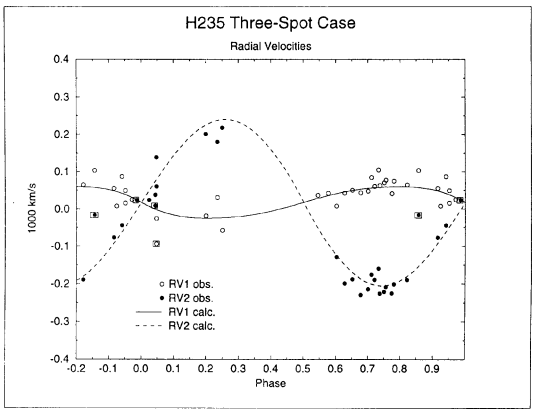


FIG. 5. Computed and observed radial velocity curves of the components of H235. The best spot model and the radial velocity data solutions are shown. The calculated radial velocity curves for the spot and nonspot models are essentially identical; the squares enclose data points accorded zero weight.

sented a new correction to the phases of the radial velocity data which was then applied, and a final run with the radial velocity data alone was performed as a check. While these results do not represent our earliest determinations and thus the actual starting point for the analyses, they represent a deeper minimum in parameter space, and thus a fit superior to all previous modeling work. Because nearly all previous modeling was performed with the same value for the phase shift parameter for both the radial velocity and photometric data, none of those runs of the full data set revealed the

TABLE 11. Radial velocity input data.

| Passband ($\lambda_0$) Φ | v/l | w | Φ | v/l | w | Φ | v/l | w | Φ | v/l | w | Φ | v/l | w |
|---|---|---|---|---|---|---|---|---|---|---|---|---|---|---|
| RV1 (.41μm): | | | | | | | | | | | | | | |
| .8209 | 0.0642 | 01 | .0469 | -.0943 | 00 | .5763 | 0.0422 | 01 | .7196 | 0.0605 | 13 | .7738 | 0.0410 | 01 |
| .8561 | 0.1032 | 01 | .1987 | -.0185 | 01 | .6016 | 0.0076 | 01 | .7366 | 0.0622 | 01 | .0469 | -.0260 | 01 |
| .9153 | 0.0548 | 01 | .2339 | 0.0305 | 01 | .6269 | 0.0424 | 01 | .7500 | 0.0696 | 01 | .2492 | -.0579 | 01 |
| .9238 | 0.0075 | 01 | .9404 | 0.0869 | 01 | .6507 | 0.0500 | 01 | .7553 | 0.0775 | 01 | .6997 | 0.0473 | 01 |
| .9709 | 0.0246 | 01 | .5445 | 0.0365 | 01 | .6759 | 0.0429 | 01 | .7803 | 0.0750 | 01 | .7100 | 0.0842 | 01 |
| .7326 | 0.1044 | 01 | .9508 | 0.0491 | 01 | .9508 | 0.0157 | 01 | | | | | | |
| RV2 (.41μm) | | | | | | | | | | | | | | |
| .8561 | -.0168 | 00 | .2339 | 0.1799 | 01 | .6507 | -.1879 | 01 | .7500 | -.2211 | 01 | .7100 | -.1760 | 01 |
| .9153 | -.0773 | 01 | .9404 | -.0447 | 01 | .6759 | -.2291 | 01 | .7553 | -.2086 | 01 | .0434 | 0.0086 | 00 |
| .0469 | 0.1382 | 01 | .2492 | 0.2181 | 01 | .6997 | -.2142 | 01 | .7738 | -.2254 | 01 | .0240 | 0.0234 | 01 |
| .0469 | 0.0599 | 01 | .6016 | -.1291 | 01 | .7196 | -.1894 | 01 | .7803 | -.2012 | 01 | .7326 | -.1596 | 01 |
| .1987 | 0.2008 | 01 | .6269 | -.1992 | 01 | .7366 | -.2258 | 01 | .8209 | -.1896 | 01 | .0430 | 0.0377 | 01 |
| .9862 | 0.0236 | | | | | | | | | | | | | |

region of parameter space represented by these subsequent analyses. This provides an instructive lesson that even the most modern and powerful tools can be defeated by small procedural detail. At the conclusion of the joint modeling, the parameters that had changed in the joint modeling were then reinserted for a final set of RV modeling, and small changes were noted in the final RV sets. These final RV results are provided in Table 13 along with an earlier converged set. Attempts to use the combined photometric and radial velocity modeling values for $q$ or $V_\gamma$ did not produce immediately convergent results for the RV data alone. On the other hand, the RV values for these quantities did not result in the best values for the combined data either. Since the fitting and $q$ value have smaller uncertainties for the combined values, the latter were adopted after all modeling was concluded.

### *3.3 Modeling Results*

After the improved phasing and radial velocity parameters determinations described in the previous section were achieved, the combined photometric and radial velocity data were again modeled together. The parameters which were adjusted were: $a, i, q, \Omega_1, T_2, L_1$, and $\Delta\phi$. Convergence was achieved for all four light curves and both radial velocity curves in four iterations, with changes to $a$ and $T_2$ being the most important. A few subsequent iterations were performed because of necessary changes to the limb-darkening coeffi-

TABLE 12. Fixed modeling parameters.

| Parameter (unit) / Component | 1 | 2 |
|---|---|---|
| | system | |
| e | 0.00 | |
| F | 1 | 1 |
| g | 1 | 1 |
| A | 1 | 1 |
| T (K) | 6500 | ...* |
| x (bol.) | 0.478 | (0.487)* |
| x (0.41μm) | 0.691 | (0.713) |
| x (0.44μm) | 0.651 | (0.671) |
| x (0.55μm) | 0.527 | (0.544) |
| x (0.64μm) | 0.447 | (0.466) |
| x (0.82μm) | 0.369 | (0.389) |

* Varied as $T_2$ was adjusted. Values shown are linearly interpolated vaues appropriate for log $g_1$ = 4.197, log $g_2$ = 4.116, and $T_2$ = 6421 K.

cients and log $g$ values (the latter are input in the DC and LC input files in WD93K93 for interpolation in the atmospheres tables).

In the nonspot treatment described in this section, there were small runs of residuals; data with residuals exceeding $2\sigma$ were subsequently treated as gross perturbations and were set to zero weight and the analyses rerun. These data are given zero weight in the binned data sets shown in Tables 6 and 11. Low weight points (less than 3 on a scale of 0 to 99) are enclosed by squares in Fig. 2. In any case, the results show only slight sensitivity to these residuals. The largest residuals were in the RV data, and consequently the major parameter change was in the semimajor axis. The effects of nulling the weights of large light curve residuals was to alter $L_1$ in $B$ and $R$ and the potential by insignificant amounts.

The results converged satisfactorily to a final solution with the figure of merit, $\Sigma w r_i^2 = 0.015\,636\,4$, corresponding to a probable error of average weight of 0.006 803. Following this convergence, the SIMPLEX-enhanced routine was used to explore parameter space to insure that the minimum found by DC was indeed the absolute minimum. The best fitting set of parameters was still that of the first DC convergence, but the simplex routine output uses the mean of the final iteration's parameters sets, all of which indicated probable errors for single average-weight observations, $e_1 = 0.006861$. The adjusted parameter values were not significantly different from those found from DC.

The results for both the final nonspot DC [Table 14(a)] and SIMPLEX [Table 15(a)] runs are tabulated for completeness. The results are not significantly different and do indeed suggest that we are at the absolute minimum of parameter space for the given set of modeled data, given the relative shallowness of the valleys of multidimensional parameter space in the convergence region. Third light contributions were explored in all passbands in early runs in both DC and SIMPLEX but no significant contribution was found in any passband.

A useful measure of the degree of overcontact is provided by the *contact parameter* (or *fillout factor*), $f$, defined here as

$$f = \frac{\Omega_i - \Omega}{\Omega_i - \Omega_0}, \tag{5}$$

where the subscripts $i$ and $o$ refer to the inner and outer Lagrangian surface potentials, obtained from the CRITOUT.TAB Roche geometry tables of Wilson (1993) for the case $F = 1.0$, the synchronous rotation case, and where $\Omega = \Omega_1 = \Omega_2$. It should be noted that $f$ as defined here does not exceed unity, and $0 \leqslant f \leqslant 1$, unlike the quantity usually referred to as the "fillout factor," which has the value 1 at the inner Lagrangian surface, and 2 at the outer. In the present case it is found that $\Omega_i = 2.2347 \pm 0.0109$, $\Omega_0 = 2.1066 \pm 0.0083$. The uncertainty in $f$ may be expressed as

$$e_f = \sqrt{\frac{(1-f)^2 e_i^2 + f^2 e_o^2 + e_\Omega^2}{(\Omega_i - \Omega_o)^2}}, \tag{6}$$

where $e_i$, $e_o$, and $e_\Omega$ are the uncertainties in $\Omega_i$, $\Omega_o$, and $\Omega$, respectively. From the DC modeling solution, $\Omega = 2.2066(106)$ and $q = 0.2005(45)$; the quantities $e_i, e_o$ are obtained form interpolating in the tables with $q \pm e_q$. With $e_i = 0.01123$, $e_o = 0.00836$, and $e_\Omega = 0.01064$, $f = 0.214(112)$. The uncertainties given in this discussion of $f$ are mean standard errors in units of the last decimal place. The Roche lobe configuration for the final model is shown in Fig. 6. The resulting absolute parameters of the system are given in Table 16. The assumed constants, $T_\odot = 5780$, $M_{\mathrm{bol}\odot} = 4.69$, $BC_{\mathrm{H235}} = 0.03$ are from Popper (1980). A three-dimensional representation of the system is shown in Fig. 7, produced with BINARY MAKER 2 software (Bradstreet 1993).

After this work was concluded, further modeling was conducted to ensure that the light curve perturbations did not affect the system and component properties. We describe this work, and the implications of Table 16 for our understanding of the system and of the cluster, in Sec. 4.

## 4. DISCUSSION

### *4.1 Spot Simulations*

The uncertainties in the derived parameters of H235 are affected by the scatter in the light curves, which is due in part to intrinsic variations in our night-to-night light curves, especially in the $I$ light curve. Figure 8 displays the *BVRI* light curves of 1989 Oct. 19 and 24 UT. Such variable light curve asymmetries are hardly unique among both eclipsing and other types of variables. The variation in the O'Connell effect (O'Connell 1951; Davidge & Milone 1984) in the $I$ passband is apparent, and in Fig. 2 very short flare-like variations are seen in the first maximum of each of the the $V$, $R$, and $I$ light curves, even though the effect on the system's mean light is nearly ignorable. From Table 8, the magnitude of the O'Connell effect in the usual sense (max II−max I) in $V$, $B-V$, $V-R$, and $V-I$, respectively, is −0.003(1), −0.003(2), −0.001(3), and −0.001(4). Thus, although the components of H235 have spectral types early enough for the atmospheres to be characterized as radiative, H235 is clearly an active system, reminiscent of the somewhat blue contact systems of the sparse globular cluster NGC 5466 (Kallrath *et al.* 1992; Milone *et al.* 1992). It should be noted, though,

TABLE 13. Radial velocity solution.

| Parameter (unit) / Model | 16a | 19 |
|---|---|---|
| a sin ($R_\odot$) | 2.675(79)* | 2.610(60)* |
| $V_\gamma$ sin i (km·s$^{-1}$) | 11.7(27) | 11.7(26) |
| $\Delta\phi$ | -0.0040(50) | -0.0045(50) |
| $q \equiv M_2/M_1$ | 0.2614(143) | 0.2486(127) |
| Fixed parameters: | | |
| i (deg.) | 58.95 | 58.70 |
| $T_{1,2}$ (K) | 6500, 6421 | 6500, 6421 |
| $\Omega_{1,2}$ | 2.2065 | 2.2065 |
| $L_1$[0.41μm] (4π) | 9.257 | 9.257 |
| $L_2$[0.41μm] (4π) | 2.860 | 2.860 |
| $\Sigma wr^2$ | 0.0006897 | 0.0006846 |
| p.e.$_1$ | 0.026081 | 0.025985 |

* Parentheses contain probable errors in units of the last decimal place for all modeled quantities. The values shown are the best WD values after $a$, $i$, $T_2$, and $\Omega$ from subsequent photometric modeling were inserted. See text for further details.

TABLE 14. (a) Differential corrections results—nonspot case.

| Parameter (unit) / Component | 1 | 2 |
|---|---|---|
| | system | |
| a ($R_\odot$) | 2.610(83)* | |
| $\Delta\phi$ | 0.0012(3) | |
| $V_\gamma$ (km s$^{-1}$) | 17.4†(41) | |
| i (deg.) | 58.70(26) | |
| $\Delta T$ (K) | | 79(25) |
| $\Omega$ | 2.0806(71) | 2.0806 |
| $q \equiv M_2/M_1$ | 0.2005(29) | |
| $L_B$ ($4\pi$) | 9.279(66) | 2.090 |
| $L_V$ ($4\pi$) | 9.360(59) | 2.124 |
| $L_R$ ($4\pi$) | 9.233(53) | 2.106 |
| $L_I$ ($4\pi$) | 9.116(49) | 2.089 |
| Derived quantities: | | |
| $R_{pole}$ (a) | 0.4934(12) | 0.2405(58) |
| $R_{side}$ (a) | 0.5389(16) | 0.2512(70) |
| $R_{back}$ (a) | 0.5636(16) | 0.2906(144) |
| $\Sigma wr^2$ | 0.0156364 | |
| p.e.$_1$ | 0.006803 | |

* Parentheses contain probable errors in units of the last decimal place.
†Assumed and unadjusted; when $V_\gamma$ is adjusted, uncertainties of other parameters increase slightly. With the best RV value for $V_\gamma$, 11.7(41), $\Sigma wr^2$ = 0.0156999 and p.e.$_1$ = 0.006817.

TABLE 14b. (b) Differential corrections results—one-spot case.

| Parameter (unit) / Component | 1 | 2 |
|---|---|---|
| | system | |
| a ($R_\odot$) | 2.610(78)* | |
| $\Delta\phi$ | 0.0007(3) | |
| $V_\gamma$ (km s$^{-1}$) | 17.4(38) | |
| i (deg.) | 58.70(24) | |
| $\Delta T$ (K) | | 79(30) |
| $\Omega$ | 2.2066(79) | 2.2066 |
| $q \equiv M_2/M_1$ | 0.2016(32) | |
| $L_B$ ($4\pi$) | 9.279(68) | 2.107 |
| $L_V$ ($4\pi$) | 9.360(60) | 2.141 |
| $L_R$ ($4\pi$) | 9.233(53) | 2.123 |
| $L_I$ ($4\pi$) | 9.116(49) | 2.106 |
| Derived quantities: | | |
| $R_{pole}$ (a) | 0.4936(13) | 0.2414(62) |
| $R_{side}$ (a) | 0.5393(17) | 0.2522(76) |
| $R_{back}$ (a) | 0.5641(17) | 0.2922(156) |
| Spot Parameters: | | |
| $\Phi$ (deg.) | 133(50) | |
| $\Lambda$ (deg.) | 299(8) | |
| $\rho$ (deg.) | 17(20) | |
| $t_f$ | 0.77(24) | |
| $\Sigma wr^2$ | 0.0144155 | |
| p.e.$_1$ | 0.006532 | |

* Parentheses contain probable errors in units of the last decimal place.

TABLE 14c. (c) Differential corrections results—two-spot case.

| Parameter (unit) / Component | 1 | 2 |
|---|---|---|
| | system | |
| a ($R_\odot$) | 2.610(76)* | |
| $\Delta\phi$ | 0.0007(14) | |
| $V_\gamma$ (km s$^{-1}$) | 17.4(36) | |
| i (deg.) | 58.70(43) | |
| $\Delta T$ (K) | | 79(57) |
| $\Omega$ | 2.207(12) | 2.207 |
| $q \equiv M_2/M_1$ | 0.2016(64) | |
| $L_B$ ($4\pi$) | 9.279(147) | 2.107 |
| $L_V$ ($4\pi$) | 9.360(132) | 2.141 |
| $L_R$ ($4\pi$) | 9.233(121) | 2.123 |
| $L_I$ ($4\pi$) | 9.116(112) | 2.106 |
| Derived quantities: | | |
| $R_{pole}$ (a) | 0.4936(22) | 0.2414(110) |
| $R_{side}$ (a) | 0.5393(31) | 0.2522(134) |
| $R_{back}$ (a) | 0.5641(37) | 0.2922(279) |
| Spot Parameters\Spot. No.: | Spot 1 | Spot 2 |
| $\Phi$ (deg.) | 133(101) | 124(246) |
| $\Lambda$ (deg.) | 299(25) | 106(263) |
| $\rho$ (deg.) | 17(71) | 15(...) |
| $t_f$ | 0.77(28) | 1.01(25) |
| $\Sigma wr^2$ | 0.0143784 | |
| p.e.$_1$ | 0.006524 | |

* Parentheses contain probable errors in units of the last decimal place.

TABLE 14d. (d) Differential corrections results—three-spot case.

| Parameter (unit) / Component | 1 | 2 |
|---|---|---|
| | system | |
| a ($R_\odot$) | 2.610(75)* | |
| $\Delta\phi$ | 0.0007(9) | |
| $V_\gamma$ (km s$^{-1}$) | 17.4(36) | |
| i (deg.) | 58.64(51) | |
| $\Delta T$ (K) | | 79(85) |
| $\Omega$ | 2.207(13) | 2.207 |
| $q \equiv M_2/M_1$ | 0.2016(42) | |
| $L_B$ ($4\pi$) | 9.279(143) | 2.107 |
| $L_V$ ($4\pi$) | 9.360(119) | 2.141 |
| $L_R$ ($4\pi$) | 9.233(103) | 2.123 |
| $L_I$ ($4\pi$) | 9.116(89) | 2.106 |
| Derived quantities: | | |
| $R_{pole}$ (a) | 0.4936(22) | 0.2414(88) |
| $R_{side}$ (a) | 0.5393(31) | 0.2522(106) |
| $R_{back}$ (a) | 0.5641(33) | 0.2922(218) |
| $\Sigma wr^2$ | 0.0139511 | |
| p.e.$_1$ | 0.006426 | |

| Spot Parameters\Spot. No.: | Spot 1† | Spot 2 | Spot 3 |
|---|---|---|---|
| $\Phi$ (deg.) | 133 | 124(31) | 66(53) |
| $\Lambda$ (deg.) | 299 | 106(19) | 99(36) |
| $\rho$ (deg.) | 17 | 15(32) | 07(9) |
| $t_f$ | 0.77 | 1.09(26) | 0.87(36) |

* Parentheses contain probable errors in units of the last decimal place.
† Assumed and unadjusted.

that the O'Connell effect may have multiple origins (Davidge & Milone 1984), so that these phenomena are not necessarily due to analogues of solar spot cycles, but may have their origins in more complex regional or global circulation activity. In any case, a series of DC and SIMPLEX spot simulations were made to explore the extent to which the derived parameters were affected by regions of apparent light enhancement or diminution. One, two, and finally, three spots were assumed to be located on the hotter component so as to match enhancements or depressions in the light curves at particular phases. The longitudes, sizes, and temperature factors were selected initially by inspection of the light curves, and the longitudes, latitudes, spot radii, and temperature factors were subsequently adjusted, one at a time for the three spots. As was done for the nonspot modeling, subsets free of strong correlations (i.e., no greater than 0.4) alone were used for adjustment. The current version of the WD program permits adjustment of only two spots at a time, so the work proceeded from convergence with one spot to convergence with two spots, and then with a third, with adjustments only to spots 2 and 3 in the last set of trials. The resulting spot parameters are included in Tables 14(b)–14(d). It is to be noted that the spot parameters are not well determined, and only the overall fit can be said to be improved, since the final errors of all system parameters are increased, in the two- and three-spot cases. Moreover, since the light

TABLE 15. (a)SIMPLEX results—nonspot case.

| Parameter (unit) / Component | 1 | system | 2 |
|---|---|---|---|
| a ($R_\odot$) | | 2.591(86)* | |
| i (deg.) | | 58.67(25) | |
| q ≡ $M_2/M_1$ | | 0.2000(31) | |
| Ω | 2.2043(76) | | 2.2043 |
| ΔT (K) | | | 83(24) |
| $L_B$ (4π) | 9.286(64) | | 2.083 |
| $L_V$ (4π) | 9.367(57) | | 2.118 |
| $L_R$ (4π) | 9.240(51) | | 2.101 |
| $L_I$ (4π) | 9.125(47) | | 2.085 |
| $R_{pole}$ (a) | 0.4938(12) | | 0.2404(60) |
| $R_{side}$ (a) | 0.5395(16) | | 0.2511(73) |
| $R_{back}$ (a) | 0.5641(16) | | 0.2906(150) |
| $V_\gamma$ (km·s$^{-1}$) | | 15.9(41) | |
| Δφ | | 0.0011(3) | |
| $\Sigma wr^2$ | | 0.0156616 | |
| p.e.$_1$ | | 0.006809 | |

* Parentheses contain probable errors in units of the last decimal place.

TABLE 15b. (b) SIMPLEX results—three-spot case.

| Parameter (unit) / Component | 1 | system | 2 |
|---|---|---|---|
| a ($R_\odot$) | | 2.571(75)* | |
| i (deg.) | | 58.52(45) | |
| q ≡ $M_2/M_1$ | | 0.2004(53) | |
| Ω | 2.2043(144) | | 2.2043 |
| ΔT (K) | | | 70(94) |
| $L_B$ (4π) | 9.269(131) | | 2.107 |
| $L_V$ (4π) | 9.354(107) | | 2.139 |
| $L_R$ (4π) | 9.228(90) | | 2.120 |
| $L_I$ (4π) | 9.116(77) | | 2.102 |
| $R_{pole}$ (a) | 0.4939(24) | | 0.2408(107) |
| $R_{side}$ (a) | 0.5396(32) | | 0.2515(130) |
| $R_{back}$ (a) | 0.5644(33) | | 0.2914(267) |
| $V_\gamma$ (km·s$^{-1}$) | | 13.5(36) | |
| Δφ | | 0.0004(8) | |

| Spot Parameters\Spot. No.: | Spot 1† | Spot 2 | Spot 3 |
|---|---|---|---|
| Φ (deg.) | 133 | 125(28) | 66(53) |
| Λ (deg.) | 299 | 106(14) | 104(35) |
| ρ (deg.) | 17 | 15(20) | 7(12) |
| $t_f$ | 0.77 | 1.11(24) | 0.88(43) |

| | |
|---|---|
| $\Sigma wr^2$ | 0.0137896 |
| p.e.$_1$ | 0.006388 |

* Parentheses contain probable errors in units of the last decimal place.
† Unadjusted in subsequent WD93K93 run (and therefore errors undetermined).

curve varies, possibly irregularly, with time, we have not made great effort to fit each and every departure in the mean light curve with spot features on both component stars. We are, however, continuing to explore the existence of spots in the system with the help of optical and infrared photometry, incomplete at this writing, and further modeling. Figure 7 shows BINARY MAKER 2 depictions for the three-spot model.

The LC93KS SIMPLEX fitting run results for the three spot case are given in Table 15(b). The sets agree, as expected, within uncertainties and suggest that the minimum represented by this particular three-spot model is the absolute minimum of parameter space. Note the location of one of the spots at the horizon of visibility in the Southern hemisphere. Since the spot solutions are nonetheless artifices at this writing, the nonspot parameters, i.e., the data of Table 14(a), were used to obtain the absolute parameters of Table 16.

### *4.2 Implications for the Nature and Evolution of H235*

The parameters of the H235 system in Table 16 give the distance modulus, both uncorrected and corrected with $A_V=3.2E_{(B-V)}=0.107(17)$, from a mean of color excess determinations, $E_{(B-V)}=0.033(5)$ (Schiller & Milone 1988), which is very close to the results adopted by Daniel *et al.* (1994), $E_{(B-V)}=0.035(5)$. The distance obtained from the derived luminosities, which are computed from derived surface areas and observed and derived temperatures of the components, further confirms the membership of H235, but places it near the center of the cluster, if, as Schiller & Milone (1988) concluded, the distance modulus for NGC 752 is 7.9(2). Whereas DS Andromedae is apparently on the far side, with $(m-M)_0=8.17(15)$ so that $r=427(30)$ pc, H235 now provides a corrected distance modulus of 7.90(10), corresponding to a distance of 381(17) pc. The average distance modulus of these two systems is 8.03(18) equivalent to an average distance of 403(34) pc.

The CMD of NGC 752 is shown in Fig. 9, adapted from Schiller & Milone (1988), which was based in turn on one from Cannon (1970). The components of H235 are indicated according to the model described in Sec. 3 by starred crosses. All the stars shown were classified as "highly probable" or "probable" members of the cluster as determined from earlier proper motion studies. Superimposed on the diagram are the theoretical isochrones of Vandenberg (1985). It is apparent from Fig. 9 that the more massive component of H235 has gained luminosity from its companion, a typical W UMa condition (see, for example, Hilditch *et al.* 1988, Fig. 3). The list of Mochnacki (1981) contains systems with components similar to those found here. Therefore, the component stars themselves are not particularly different from those of other contact systems in the field.

If the system was neither formed subsequent to cluster formation, nor dynamically affected to any significant extent by collisions, the hypothesis that systems with initial periods

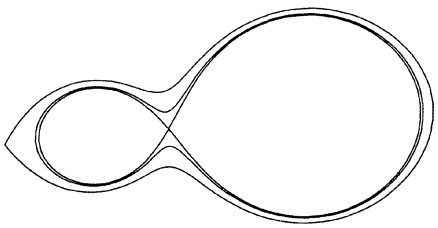

FIG. 6. An approximation to the Roche lobe configuration of the H235 system, produced with the package BINARY MAKER 2, by D. H. Bradstreet.

of order 2 days evolve into contact systems through angular momentum loss would find mild support in this contact system in a cluster of intermediate age. However, the kinematic age of contact systems in the field is much greater than the cluster and thus of the binary. In fact, a dynamical argument can be presented that the system is likely to have been hardened; that is, its dynamical evolution towards merger accelerated, as a consequence of interaction with other cluster members.

One would expect that while a particular collision in any cluster is certainly not impossible, the relative sparseness of this open cluster would make the probability of collisions vanishingly small. This is not entirely true.

Simple two-body encounter theory suggests that the number of encounters is

$$N_{\rm enc}=3.22\times10^{-6}D^2n\nu\tau, \quad (7)$$

where $D$ is the impact parameter in parsecs, $n$ is the population density in number of stars per pc$^3$, and $\nu$ is the relative speed of approach, in km s$^{-1}$, and $\tau$ is the lifetime of the ensemble in years, which we take as 2 Gyr. The results depend strongly on the assumed conditions. If we assume $n=1.24$ and $D=3.1$ pc (the present density and radius of the cluster core according to Artyukhina & Kholopov 1965), and $\nu=\sqrt{[3\cdot(V_\gamma-\langle V\rangle)]}\simeq1$ km s$^{-1}$, where $\langle V\rangle=9$ km s$^{-1}$, according to Rebeirot (1970), $N_{\rm enc}\approx7.7\times10^4$, or about one collision per $2.6\times10^4$ yr, on average. If the impact parameter is set equal to a more conservative value of $10a$, and $D=25R_\odot=0.117$ AU$=5.6\times10^{-7}$ pc, $N_{\rm enc}\approx2.6\times10^{-9}$ over the age of the cluster. Thus, this type of strong interaction is highly unlikely, although if we allow for *all* potential progenitors (say ~100), adjust the impact parameter for gravitational focusing (Leonard 1994), and set initial conditions appropriate to a binary at $P\sim2$ d, so that $D=16.7$ AU, then $N_{\rm enc}$ increases to $\sim5\times10^{-3}$.

Nevertheless, interactions *are* likely to have occurred, especially in the past, when the cluster was richer, as we can show by considering gravitational interactions. Consider the interaction between a star and a succession of target stars. Over the dynamical collision time, $\tau_D$, the time for the orbit of a star to be altered by ~1 rad due to many successive, small angular shifts in direction of order $\langle\psi^2\rangle$, can be written

$$\Sigma\psi^2=N_{\rm enc}\langle\psi^2\rangle \quad (8)$$

and since it may be shown that

$$\langle\psi^2\rangle=4\mu^2/(v^4D^2) \quad (9)$$

for a hyperbolic collision, we may combine (7), (8), and (9), and now set $\tau=\tau_D$ to obtain

$$\tau_D=1.66\times10^{18}v^3/(4\pi\mu^2n). \quad (10)$$

In the present case, the time for the orbit to be irretrievably altered, $\tau_D=8\times10^8$ yr, less than half the age of the cluster. Because they are so much more likely than strong interactions, weak interactions may have important effects on the orbital properties of a binary system. Leonard (1994) indicates that a hardening collision of an already hard binary is more likely to result in recoil ejection of the binary from the cluster altogether, than in a mere decrease of the binary's semimajor axis; alternatively, an increase in eccentricity, which is far easier to attain than a large decrease in semimajor axis in collisions, followed by tidal circularization of the orbit, can result in a tight binary that remains bound to the cluster.

TABLE 16. Absolute parameters of H235.

| Parameter (unit) / Star | 1 | system | 2 |
|---|---|---|---|
| a ($R_\odot$) | | 2.610(124)* | |
| M ($M_\odot$) | 1.176(173) | 1.411(176) | 0.236(35) |
| <R> ($R_\odot$) | 1.391(2) | | 0.680(9) |
| $f$ | | 0.214(112) | |
| T (K) | 6500(150)† | | 6421(155) |
| $\mathcal{L}$ ($\mathcal{L}_\odot$) | 3.094(293) | | 0.704(85) |
| $M_{bol}$ | 3.464(103) | | 5.071(132) |
| $M_V$ | 3.49(10) | 3.41(11) | 5.10(13) |
| $<V_{max}>$ | 11.499(7) | 11.277(7) | 13.109(15) |
| $<B-V>_{max}$ | 0.444(13) | 0.445(9) | 0.452(24) |
| $V-M_V$ | | 8.01(10) | |
| E(B-V) | | 0.033(5)† | |
| $(V-M_V)_0$ | | 7.90(10)** | |
| r (pc) | | 381(17) | |
| $V_\gamma$(km s$^{-1}$) | | 11.7(27) | |
| $V_T$ (km s$^{-1}$) | | 17.7(36) | |
| $V_{Space}$(km s$^{-1}$) | | 21.2(45) | |

* Parentheses contain standard errors in units of the last decimal place.
† assumed and unadjusted; uncertainty estimated.
** R =3.2(2) assumed, to give $A_V$ = 0.106(17)

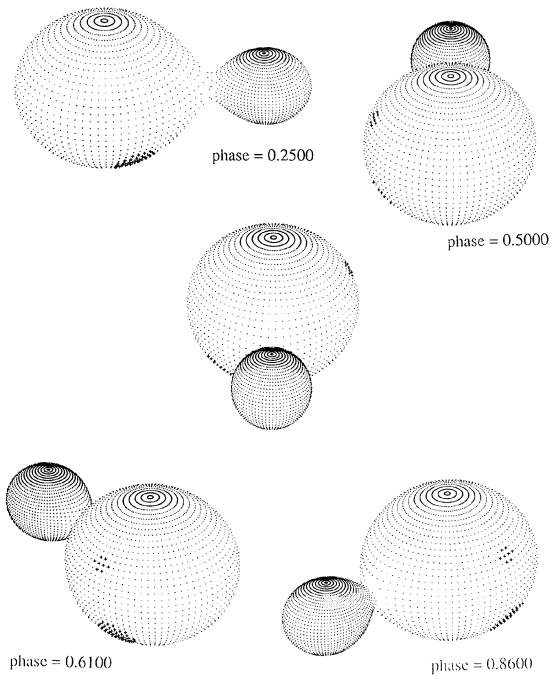


FIG. 7. Three-dimensional representations of the contact system H235 [three-spot model of Table 14(d)] at selected phases, displayed around the appearance of the system at phase 0.000, produced with the BINARY MAKER 2 software package (Bradstreet 1993). Note the broad visibility of the spots.

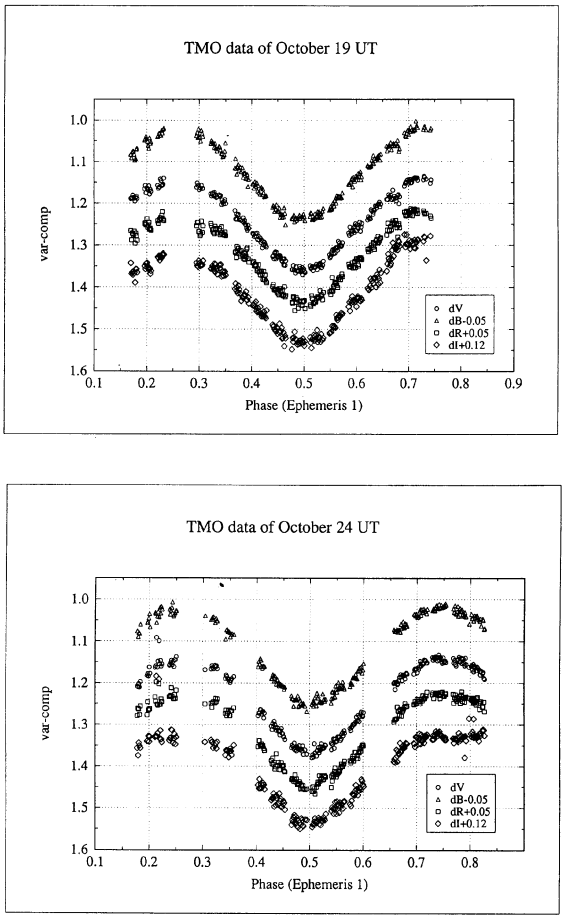


FIG. 8. The Table Mountain *BVRI* light curves of 1989 Oct. 19 and 24 UT. The variation in the *I* passband O'Connell effect is apparent.

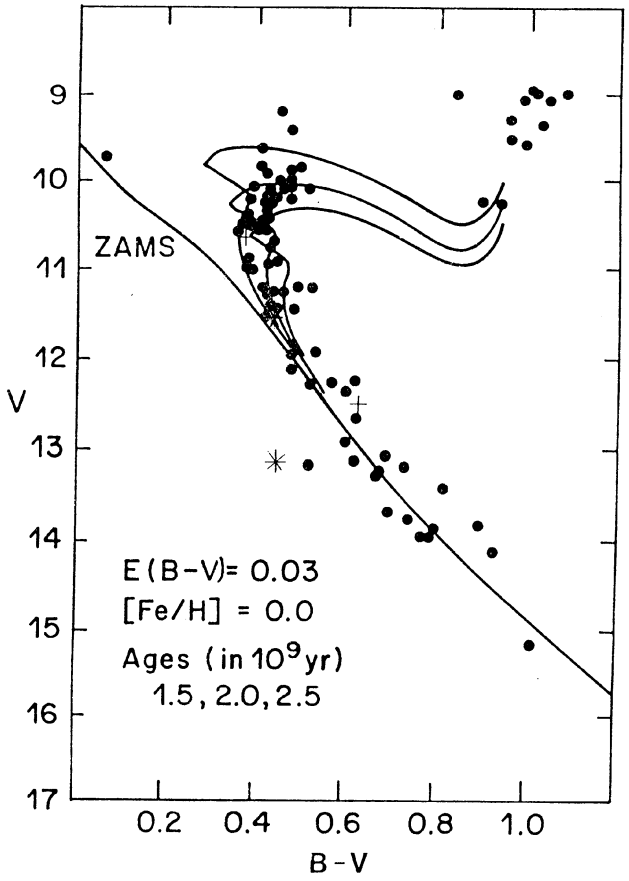


FIG. 9. The color–magnitude diagram of the cluster NGC 752 indicating the components of DS And and H235 by crosses and for the latter, superimposed "X's."

In addition, as has been noted often, a diminution of the semimajor axis *can* come about as a result of orbital evolution. If we adopt Vilhu's (1982) evolution scenario for contact binaries, the period evolution depends on the power, $\alpha$, in the angular momentum loss equation,

$$\frac{dJ_{\rm spin}}{dt} \approx -4\times10^{41}\left(\frac{1}{3}P_{\rm init}\right)^{-\alpha}, \qquad (11)$$

where $\alpha=3$ for single stars. For a range $1<\alpha<3$, the corresponding initial period range is about $1<P_{\rm init}<2.5$ d for two stars of solar mass to reach contact in an interval of ~2 Gyr. This scenario assumes no collisional effects superimposed on the evolution, so that the combination would appear to account for the existence of a contact system of intermediate contact parameter. However, Kraicheva *et al.* (1979) note the existence of a cutoff period ~2 $^{\rm d}$, a condition which constrains the initial period, in the absence of collisions, rather tightly. The likelihood of collisions, on the other hand, both relieves the constraint and makes impossible precise depiction of the binary's evolution.

As Eq. (10) indicates, the probability of collision depends on time and stellar density, and, as we describe below, there is evidence that $n$ was higher in the past than at present. Therefore, after the initial epoch, the collision rate would have decreased, so that hardening collisions of any type are more likely to have occurred early in the cluster's history.

Thus, we can tentatively assign the cluster's age to this particular system, if indeed the cluster was formed coevally. With this caveat, H235 joins a small number of contact systems in open clusters for which age is determinable.

Can it, though, be assumed that the cluster's present star population formed coevally? There is evidence that present cluster conditions have not always applied. Eggen & Iben (1989) argue that more than one episode of star formation must have occurred in NGC 752 on the basis of isochrone fittings to at least two groups of objects, which suggest to them principal bursts of star formation at ages of 1.5 and 2.5 Gyr. They claim that the hotter component of DS Andromedae falls on the 1.5 Gyr isochrone, and that two other objects, H110 (a "deviant giant") and H209 (a blue straggler) fall near an isochrone of 0.8 Gyr. If these deductions are even partly reliable, the desired relationship between chronological age and binary development stage cannot be realized readily. Francic's (1989, Fig. 1) proper motion vector point diagram for NGC 752 suggests at least two groups of stars, separated kinematically. Finally, there is evidence for a mag-

nitude turnover at $M_{pg}=3.0$ in the luminosity function of this cluster (Platais 1991; Francic 1989) implying that the faint, low mass stars of this cluster have been lost by evaporation. Using a relation for a cluster's relaxation time, $\tau_r$ from Spitzer & Hart (1971), namely,

$$\tau_r=\frac{8.5\times10^5 N R_{1/2}^{1.5}}{N M_T^{1/2}\log N}, \quad (12)$$

Francic (1989) notes that the evolution age (taken as 2 Gyr) is several hundred times larger than the relaxation time and that very few faint stars have membership probabilities greater than 0.5. The anomaly may be explained by the ejection of the low mass systems through collisional interactions, although this begs the question as to why this particular intermediate-age cluster has undergone such wholesale ejections while others have not to the same degree. In any case, the conclusion supports the idea that dynamical effects should have occurred early in the cluster's history. The multiple starburst theory suggests, however, that the history is even more complex.

Leaving aside questions about the causes of such starbursts, there are some arguments to be made against the multiple starburst theory. First, the study by Friel & Janes (1993) of 24 open clusters with ages greater than 1 Gyr suggests that some measure of uniformity can be found among the stars they studied in NGC 752. The observed average metallicity for NGC 752 {[Fe/H]=−0.162(16)} from their analyses of nine giants (all highly probable members), places them squarely on the relation between [Fe/H] and galactocentric distance. Friel and Janes did not find any strong correlation of [Fe/H] and age, but for the seven clusters which they studied with ages 2 Gyr and younger, they found that the difference in metallicity as determined by magnesium lines as opposed to iron lines was represented by the relation: $\Delta[\mathrm{Fe/H}]_{\mathrm{Mg-Fe}}=-0.45(8)$. Again, their sample from NGC 752 falls in the middle of this relation at −0.42(17), suggesting an age no later than about 2 Gyr for the sample. The modest dispersion in [Fe/H] in this cluster also argues, though weakly, against the relatively unlikely circumstance of collisions with similar-composition dust clouds. Second, the isochrone studies of individual objects, the masses of which have not been obtained, must be accepted cautiously, especially if the objects are peculiar. Most critically, the extensive analysis of the properties of the DS And primary star by SM88 suggests an age of 2.0(2) Gyr (see their Fig. 10) for this component, not 1.5 Gyr as argued by Eggen & Iben (1989), questions about convective overshoot notwithstanding. In addition, the use of a blue straggler to determine an age is certainly moot since the origin of blue stragglers is, at this writing, still not known, and, of course, neither are their masses. Stryker (1993) concludes in her summary that more than one mechanism to produce blue stragglers is likely. If, as many (but not all) astronomers believe, blue stragglers are merged binaries, there is still a question of the time scale—the merger may be purely a result of some lengthy angular momentum loss mechanism or the process may be accelerated by a hardening collision with another binary. Thus, the history of such an object is too complex to predict its age with any certainty, in our view. Summing up, at present there is no compelling evidence *from evolution arguments alone* for multiple starburst occurrences in NGC 752, and thus to doubt the coeval nature of H235, DS And, and other confirmed members of NGC 752. A similar conclusion above the coeval nature of the stars of NGC 752 is arrived at independently by Daniel *et al.* (1994). Nevertheless, weak interactions in H235's history are likely and therefore the initial conditions of the system cannot be determined with any certainty.

## 5. CONCLUSIONS

H235 is a contact system in the intermediate age open cluster NGC 752. We have not attempted to model the evolution of this system in the work described here, but the age is expected to be coeval with other stars of the cluster, namely, ~1.7–1.9 Gyr. This result is confirmed to some extent, first, by Francic's (1989) conclusion that NGC 752 has an evolutionary age much greater than its relaxation time, second, by the relation found by Friel & Janes (1993) between metallicity and age as derived from Fe and Mg indices of clusters no older than 2 Gyr. Similar conclusions are reached by Daniel *et al.* (1994) on the basis of all available evidence.

An age of nearly 2 Gyr is somewhat surprising for a contact binary, in light of kinematic studies of field stars, such as that of Guinan & Bradstreet (1988), which suggest greater ages (8–10 Gyr), on the whole, for these systems, many of which, however, have somewhat smaller contact parameters than does H235 (e.g., RW Com and TY Boo). Contact systems have been observed in globular clusters (such as NGC 5466 and M71) and in other open clusters. Guinan and Bradstreet summarize the situation in galactic open clusters as of 1988, and more recently, Rucinski (1994) has done so; both summaries note the interesting case of the W-type W UMa system TX Cancri in M44, which is less than ~1 Gyr old; but as a rule, the evidence is that contact systems appear in clusters older than 2 Gyr. The disparity in age between H235 and almost all other contact systems therefore supports either an unusually short initial period or a collisional path to faster evolution for both H235 and for TX Cnc. As we note in Sec. 4, collisions are likely to have played a more important role early in the cluster's history but continuing weak interactions can be expected to have contributed to the orbital evolution of H235 through angular momentum loss.

The contact parameter (0.22±0.11) of H235 suggests that it is intermediate in its evolution toward coalescence and thus may represent a fiducial point in the study of close binary star evolution. It is interesting to note that the expected lifetime of contact (Vilhu 1982) is between 0.1 and 1.0 Gyr, so that the time for H235 (and TX Cnc) to achieve contact had to be even shorter than the cluster's lifetime.

Ignoring collisional interactions, this situation constrains the initial period to be close to or less than the 2 $^{d}$ cutoff proposed by Kraicheva *et al.* (1979).

The investigation of many systems in galactic clusters is required to resolve the question of the evolution of contact binaries. Therefore, the current active searches for binaries in clusters assume great importance.

For the future, we have begun to obtain optical and infrared images of H235 and of NGC 752 to seek further clues of the evolution of this interesting cluster and of its component stars, and Latham's group is obtaining precision radial velocities (Latham *et al.* 1992; Latham 1994), which should further improve the modeling. We are also conducting an extensive search for additional variables in open and globular clusters; in such an extensive enterprise, collaborators are welcome.

This paper has had precursors in University of Calgary graduate and undergraduate research projects on the radial velocity and SIMPLEX modeling (by BJAS) and on the CCD data (by JRM), but carried out on less comprehensive and consistent sets of data. The authors would like to thank the TACs and directors of the Table Mountain, Mt. Laguna, and Dominion Astrophysical Observatories. The writing of this paper began while E.F.M. was a visitor at the CFHT Corporation Headquarters in Waimea, Hawaii in January and February 1993, and was continued at DAO in April and May, and at the Ruhr Universität Bochum, Germany in July and August 1993. The hospitality and assistance provided by each of these institutions is warmly appreciated. Horst Fichtner assisted with programing expertise. Critical readings of this work by Albert Linnell and Peter Leonard are greatly appreciated and have led to revisions of sections of the work. The comments of our referee about the radial velocity modeling have been invaluable and have strongly improved the work. D. Terrell kindly provided a useful program to interpolate bilinearly among Van Hamme's limb-darkening tables. This work was supported by NSERC and U. of Calgary Research grants and a DAAD German travel fellowship to E.F.M., a University of Calgary Post-Doctoral Research Fellowship to C.R.S., a Northwest Area Foundation Grant of the Research Corporation to S.J.S., and a German–Canadian Travel Grant to the University of Calgary and the University of Bonn by GKSS, Geesthacht, FRG, and a NATO grant awarded to Prof. S. R. Sreenivasan, both for J.K.'s travel are all acknowledged with gratitude.

## REFERENCES

Abt, H. A., & Biggs, E. S. 1972, Bibliography of Stellar Radial Velocities (Latham Process Corp, N. Y.)
Artyukhina, N. M., & Kholopov, P. N. 1965, AZh, 41, 743 (Trans. in SvA-AJ, 8, 590)
Bradstreet, D. H. 1993, in Light Curve Modeling of Eclipsing Binary Stars, edited by E. F. Milone, (Springer, New York), p. 151
Breinhorst, R. A., Kallrath, J., & Kämper, B. C. 1989, MNRAS, 241, 559
Cannon, R. D. 1970, MNRAS, 150, 111
Crawford, D. L., & Barnes, J. V. 1970, AJ, 75, 946
Daniel, S. A., Latham, D. W., Mathieu, R. D., & Twarog, B. A. 1994, PASP, 106, 218
Davidge, T., & Milone, E. F. 1984, ApJS, 55, 571
Dreschel, H., Lorenz, R., & Mayer, P. 1989, A&A, 221, 49
Ebbighausen, E. G. 1939, ApJ, 98, 431
Eggen, O., & Iben, I. 1989, AJ, 97, 431
Francic, S. P. 1989, AJ, 98, 888
Friel, E. D., & Janes, K. A. 1993, A&A, 267, 75
Guinan, E. F., & Bradstreet, D. H. 1988, in Formation and Evolution of Low Mass Stars, edited by A. K. Dupree and M. T. Lago (Kluwer, Dordrecht), p. 345
Hardy, E. 1979, AJ, 84, 319
Heinemann, K. 1926, ANac, 227, 193
Hilditch, R. W., King, D. J., & McFarlane, M. 1988, MNRAS, 231, 341
Hill, G. 1982, Publ. DAO, 16, 59
Johnson, H. L. 1953, ApJ, 117, 356
Kallrath, J. 1987, Diplomarbeit (Astronomische Institute, Bonn)
Kallrath, J. 1993, in Light Curve Modeling of Eclipsing Binary Stars, edited by E. F. Milone (Springer, New York), p. 39
Kallrath, J., & Linnell, A. P. 1987, ApJ, 313, 346
Kallrath, J., Milone, E. F., & Stagg, C. R. 1992, ApJ, 389, 590
Kraicheva, Z. T., Popova, E. L., Tutokov, A. V., & Yungelson, L. R. 1979, Astron. Zh., 58, 520
Kurucz, R. L. 1979, ApJS, 40, 1
Kurucz, R. L. 1993, in Light Curve Modeling of Eclipsing Binary Stars, edited by E. F. Milone (Springer, New York), p. 93
Landolt, A. U. 1983, AJ, 88, 439
Latham, D. W. 1994, personal communication
Latham, D. W., Daniel, S. A., Mathieu, R. D., & Twarog, B. A. 1992, in The Formation and Evolution of Star Clusters. ASP. Conf. Series, No. 13, p. 275
Leach, R. W. 1992, private communication
Leonard, P. J. 1994, private communications
Milone, E. F., & Schiller, S. J. 1988, in The Extragalactic Distance Scale, edited by S. van den Burgh and C. J. Pritchett (BYU, Salt Lake City), p. 182
Milone, E. F., & Schiller, S. J. 1991, in The Formation and Evolution of Star Clusters, edited by K. Jones (BYU, Provo), p. 427
Milone, E. F., Groisman, G., Fry, D. J. I., & Bradstreet, D. H. 1991, ApJ, 370, 677
Milone, E. F., Stagg, C. R., & Kurucz, R. L. 1993, ApJS, 79, 123
Milone, E. F., Stagg, C. R., McVean, J., Sugars, B. J. A., & Schiller, S. J. 1992, in Evolutionary Processes in Interacting Binary Stars, edited by Y. Kondo, p. 475
Milone, E. F., Chia, T. T., Castle, K. G., Robb, R. M., & Merrill, J. E. 1980, ApJS, 43, 339
Mochnacki, S. W. 1981, ApJ, 245, 650
O'Connell, D. J. K. 1951, Riverview Publs., 2, 85
Pilachowski, C. A., Willmath, D. W., Halbedel, E. M., Mathieu, R. D., Hobbs, L. M., Milkey, R. W., & Saha, A. 1986, PASP, 98, 1321
Platais, I. 1991, A&AS, 87, 69
Popper, D. M. 1980, ARA&A, 18, 115
Rebeirot, E. 1970, A&A, 4, 404
Rohlfs, K., & Vanýsek, V. 1961, Hamburg Astronom. Abh., 5, No. 11
Roman, N. G. 1955, ApJ, 121, 454
Rucinski, S. M. 1994, PASP, 106, 462
Ruprecht, J. Balázs, B., & White, R. E. 1988, Catalogue of Star Clusters and Associations (Akadémiai Kiadó, Budapest)
Schiller, S. J. 1986, Ph.D. thesis, The University of Calgary
Schiller, S. J., & Milone, E. F. 1988, AJ, 95, 1466 (SM88)
Spitzer, L., & Hart 1971, ApJ, 164, 399
Stagg, C. R., Milone, E. F., Kurucz, R. L., & Terrell, D. 1995, in preparation
Stock, J. 1985, RMxA, 11, 103
Stryker, L. L. 1993, PASP, 105, 1081
Twarog, B. A. 1983, ApJ, 267, 207
VandenBerg, D. A. 1985, ApJS, 58, 711

Van Hamme, W. 1993a, AJ, 106, 2096
Van Hamme, W. 1993b, personal communication
Vilhu, O. 1982, A&A, 109, 17
Wade, R. A., & Rucinski, S. M. 1985, ApJS, 60, 471
Walker, R. L., & Chambliss, C. R. 1990, AJ, 100, 233
Wilson, R. E. 1992, Documentation of Eclipsing Binary Computer Model, (University of Florida, Gainesville)
Wilson, R. E., & Biermann, P. 1976, A&A, 48, 349